AN ABSTRACT OF THE THESIS OF

Boonsong Siwamogsatham (Name) for the Doctor of Philosophy (Degree)

in General Science (Physical Science) (Major) presented on May 5, 1971 (Date)

Title: NUCLEAR LEVEL STRUCTURE OF ^{101}Ru FROM THE 14.0 MINUTE ^{101}Tc DECAY

Abstract approved: Redacted for Privacy

Dr. Harry T. Easterday

The nuclear level structure of ^{101}Ru has been investigated through the decay of 14.0 minute ^{101}Tc produced by thermal neutron irradiation of molybdenum targets. Gamma-ray energies and relative intensities have been measured with the high resolution Ge(Li) spectrometers. Based on the energy sum and the intensity balancing, a consistent level scheme of ^{101}Ru is proposed. Origins of spin-parity of the levels in ^{101}Ru are discussed on the ground of de-Shalit weak coupling core excitation model. The results of this study are compared with the recent extended quasiparticle phonon coupling calculations.

The gamma-ray energies and relative intensities emitted in the decay of 14.6 minute ^{101}Mo have also been measured. Several new gamma transitions and level energies have been observed, and a new level scheme of ^{101}Tc is proposed.

Nuclear Level Structure of ^{101}Ru From the 14.0 Minute ^{101}Tc Decay

by

Boonsong Siwamogsatham

A THESIS

submitted to

Oregon State University

in partial fulfillment of
the requirements for the
degree of

Doctor of Philosophy

June 1971

APPROVED:

Redacted for Privacy

Professor of Physics

in charge of major

Redacted for Privacy

Chairman of Department of General Science

Redacted for Privacy

Dean of Graduate School

Date thesis is presented May 5, 1971

Typed by Barbara Eby for Boonsong Siwamogsatham

ACKNOWLEDGEMENT

The author wishes to express his sincere gratitude to Dr. Harry T. Easterday, the major professor, for his judicious advice and continued assistance throughout the course of this study, and to Dr. B. Kalakitcha, the rector of Khon-Kaen University, for his continued encouragement and support.

Special thanks are expressed to Dr. Larry Schecter for his assistance and acting as major professor during Dr. Easterday's sabbatical leave at the University of California Lawrence Radiation Laboratory, Livermore; to Dr. Timothy G. Kelley and Dr. Earl Barnes for valuable discussions; and Dr. Chih H. Wang, Director of Radiation Center, and the OSU reactor staff for target irradiations.

The financial support by His Majesty's Government of Thailand through a scholarship program of the Thai Civil Service Commission is gratefully acknowledged.

TABLE OF CONTENTS

LIST OF FIGURES

LIST OF TABLES

NUCLEAR LEVEL STRUCTURE OF ^{101}Ru FROM THE 14.0 MINUTE ^{101}Tc DECAY

INTRODUCTION

Gamma-ray spectroscopy has contributed valuable information as to the progressively increasing knowledge in the field of nuclear structure physics. A primary concern of low energy experimental nuclear spectroscopy is the determination of the excited and ground state properties of nuclei such as angular momentum, energy, parity and electromagnetic lifetime.

In the pre-semiconductor detector period, gamma-ray spectroscopy had long been handicapped by the poor balance among three important factors: the resolving power, which places a limit on the complexity of spectrum that can be examined; the detection efficiency, which determines the strength of the source required; and the speed of data accumulation, which is of great importance when work is done with short-life isotopes. The introduction of the curved-crystal focussing spectrometer by DuMond (24) in 1947 made possible the precision measurement of gamma-ray energies. The most recent improvement of a curved-crystal diffraction spectrometer was reported by Raeside (77). But exceedingly low efficiency has a limited application of this type of spectrometer. At the other extreme, very high detection efficiency with moderate resolution, are gamma-ray

spectrometers utilizing NaI(Tℓ) scintillation detectors which were developed in the late 1940's (8).

In the pre-1960 period, the NaI(Tℓ) crystal was the most successful and popular gamma-ray detector. This scintillator revolutionized gamma-ray spectroscopy because it provided an energy-sensitive spectrometer with high detection efficiency, moderately good resolution, excellent timing characteristics and was a multi-channel type device. The contribution of scintillation spectrometers to the field of nuclear physics during such a period has been well understood. However, as the field of nuclear-structure physics progressed and the realization emerged of the great complexity of nuclear level schemes, it was obvious that the scintillation spectrometer was no longer capable of the task that lay before nuclear spectroscopists.

During the past decade a new device has emerged to essentially replace the NaI(Tℓ) scintillation detector in spectroscopy. This device is the lithium-drifted, Ge(Li) detector. The first published report of the use of 0.2 c. c. germanium lithium drifted p - i - n detector for gamma-ray spectroscopy is that by Freck and Wakefield (32) in 1962. While the early devices were small, essentially less than 1.0 c.c., a method had later been described by several authors (27, 55, 56, 57, 61, 87) how practical detectors having active volumes up to 54 c. c. could be constructed. Moreover, various companies are now commerically manufacturing Ge(Li) detectors of various

sizes and shapes at relatively reasonable cost. Therefore, a particularly favorable compromise between the three critical criteria of gamma-ray spectrometer has finally been achieved and the gamma-ray spectrometer employing a Ge(Li) detector is now occupying the "middle role" between the very high resolution instruments whose applications are limited by very low efficiency and the very efficient scintillation spectrometer whose applications are limited by poor resolution. A comparison of the observed resolution (FWHM)[1]-energy relationship for typical nuclear spectrometer using NaI(Tℓ), Ge(Li) and diffraction crystal detectors is shown in Figure 1. In addition, Figure 2 illustrates the approximate total full energy peak absorption efficiency - energy relationship of some typical nuclear spectrometers, for comparison. It is generally accepted that Ge(Li) detector is now revolutionizing all fields in which quantitative gamma-ray data are of crucial experimental importance.

Two Ge(Li) detectors were used in this investigation, one of which is a small planar type detector having an active volume of 1.2 c. c., the other is a large trapezoidal type with 25 c. c. active volume. The former was used for preliminary studies of ^{101}Tc decay and the later was employed in the quantitative investigation of gamma rays emitted in the decay of this isotope.

---

[1] (FWHM) means full width of the energy peak at half maximum expressed in kiloelectron volts.

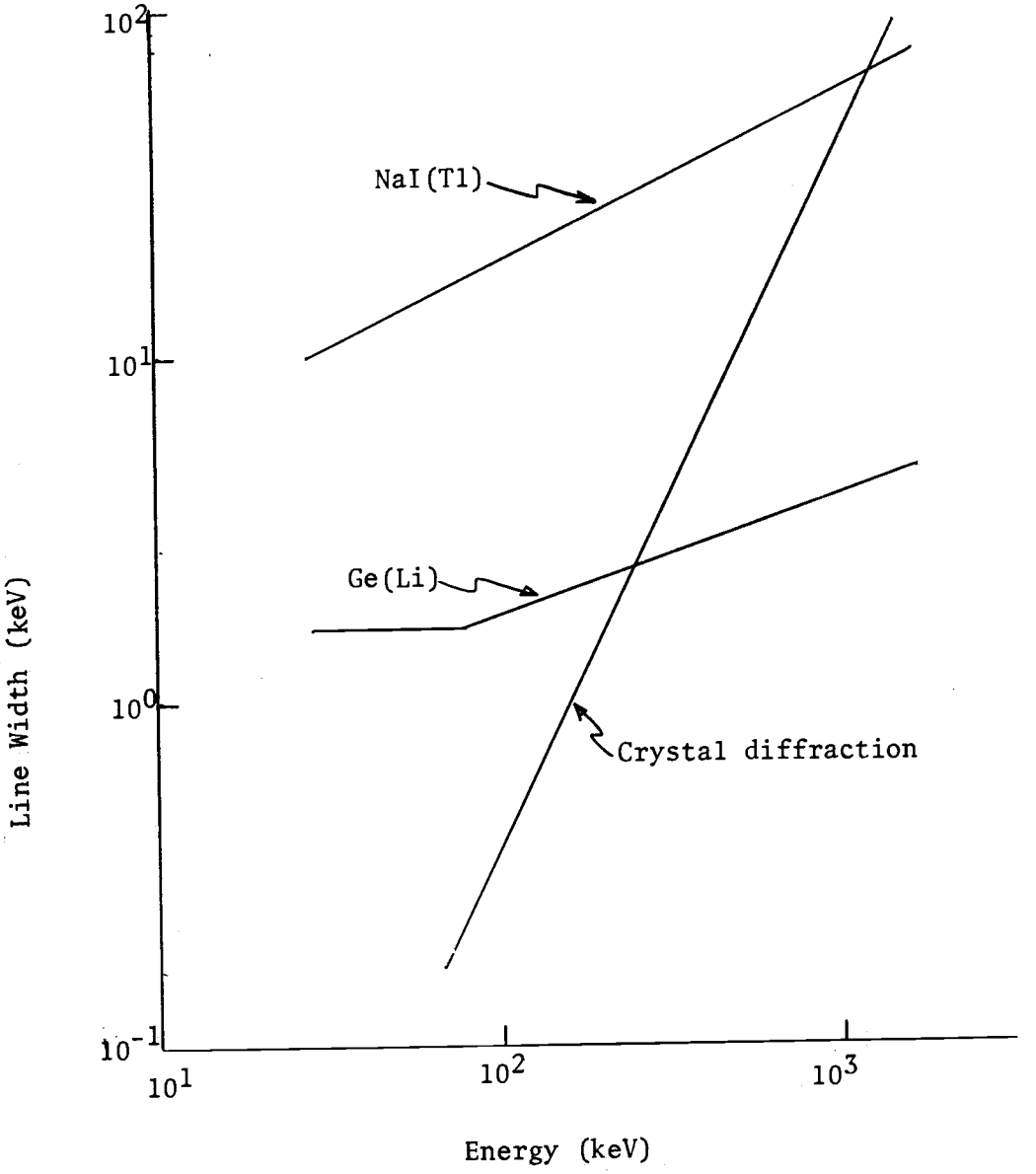

Figure 1. Comparison of resolution-energy relationship for nuclear spectrometer using NaI(Tl), Ge(Li) and crystal diffraction detectors, adapted from Hollander (41).

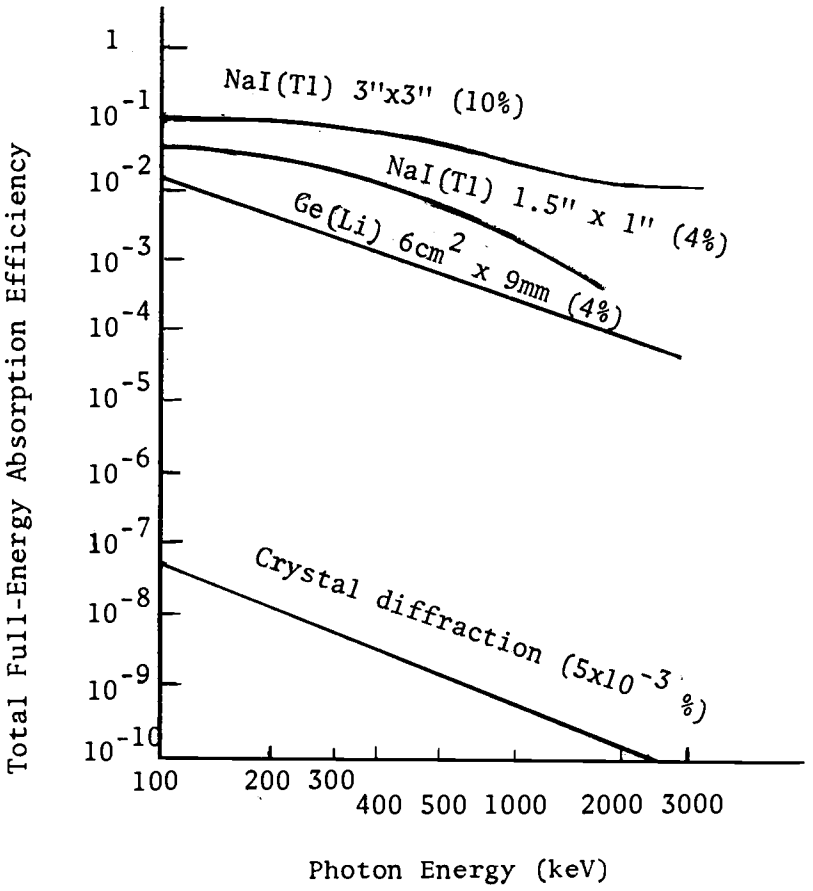

Figure 2. Comparison of practical efficiencies of NaI(Tl), Ge(Li) and crystal diffraction spectrometers, adapted from Hollander (41). Assumed solid angles are given in parenthesis.

Nuclei of ^{101}Tc undergo beta-decay to the excited states of ^{101}Ru with a half-life of 14.0 minutes (71). Prior to the development of the Ge(Li) detector the most important investigations of the decay of ^{101}Tc were carried out with the use of beta and scintillation spectrometers by Martin et al. (59) and O'Kelley et al. (71). Very recent NaI(Tℓ) - NaI(Tℓ) gamma-ray coincidence studies of the ^{101}Tc decay were carried out by Cretu and Funke (19), and the first published ^{101}Tc decay scheme is shown in Figure 3. The first use of a small Ge(Li) detector for the investigation of ^{101}Tc is that in 1965 by Aras et al. (2), who used a planar detector having active volume of 0.6 c. c. in their gamma spectrometer. However, the findings of their studies showed, among other things, the inadequacy of both resolution and efficiency of the detector to unfold the complex ^{101}Tc gamma spectrum. This, then, is the purpose of this investigation, to reexamine the decay of ^{101}Tc with high resolution Ge(Li) detectors with sufficient efficiency in order to determine if the nuclear level structure of ^{101}Ru indicated in the presently accepted decay scheme (53) as shown in Figure 4 can be improved.

Levels of ^{101}Ru below 639 keV are also populated by electron-capture of ^{101m}Rh with 4.3 day half-life and by 3.0 year ^{101g}Rh. A thorough investigation of low-lying levels of ^{101}Ru from the decay of ^{101}Rh have been carried out (3, 17, 26) with the aid of small volume planar type Ge(Li) detectors and magnetic spectrographs. Coulomb

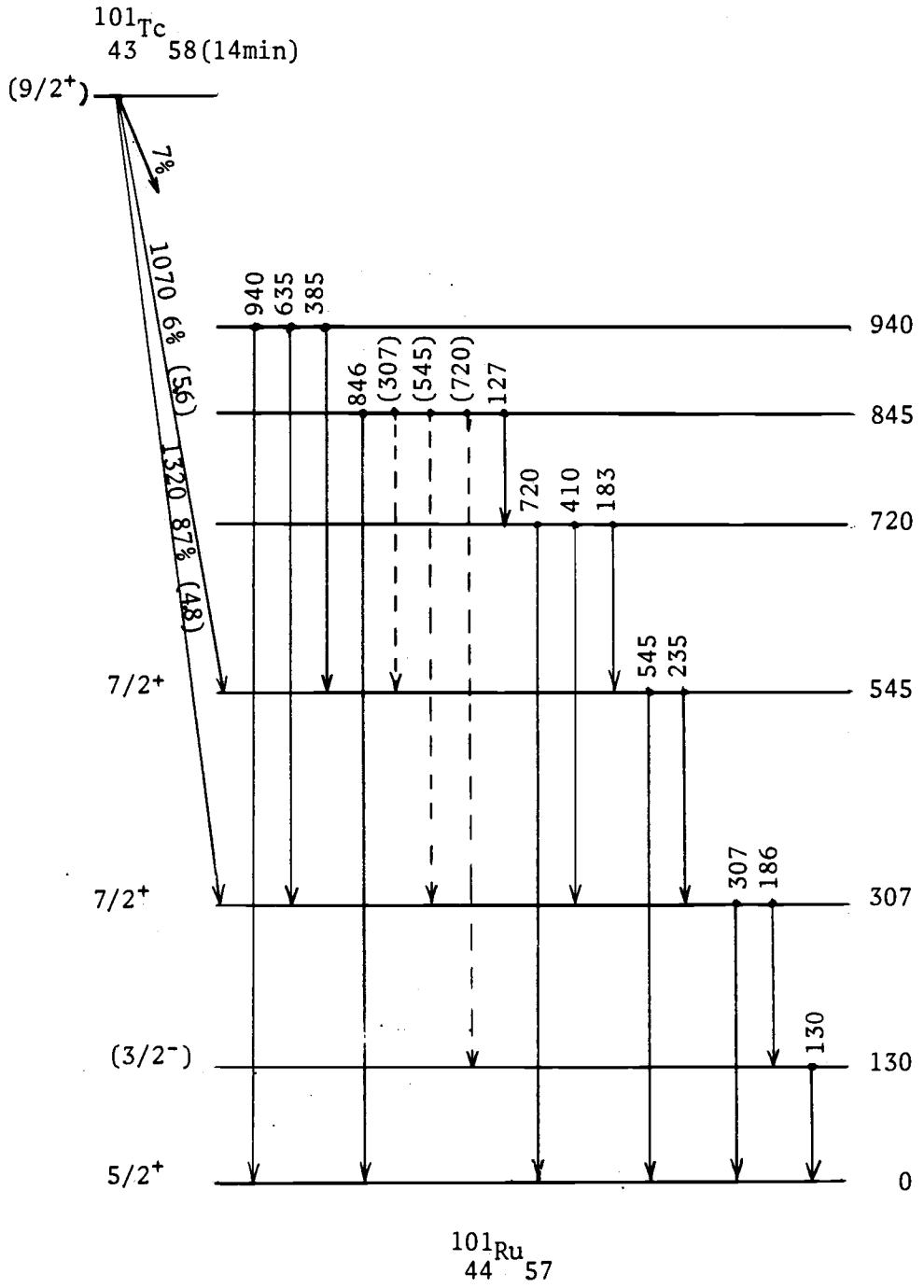

Figure 3. Decay scheme of ^{101}Tc, proposed by Cretu and Funke (19).

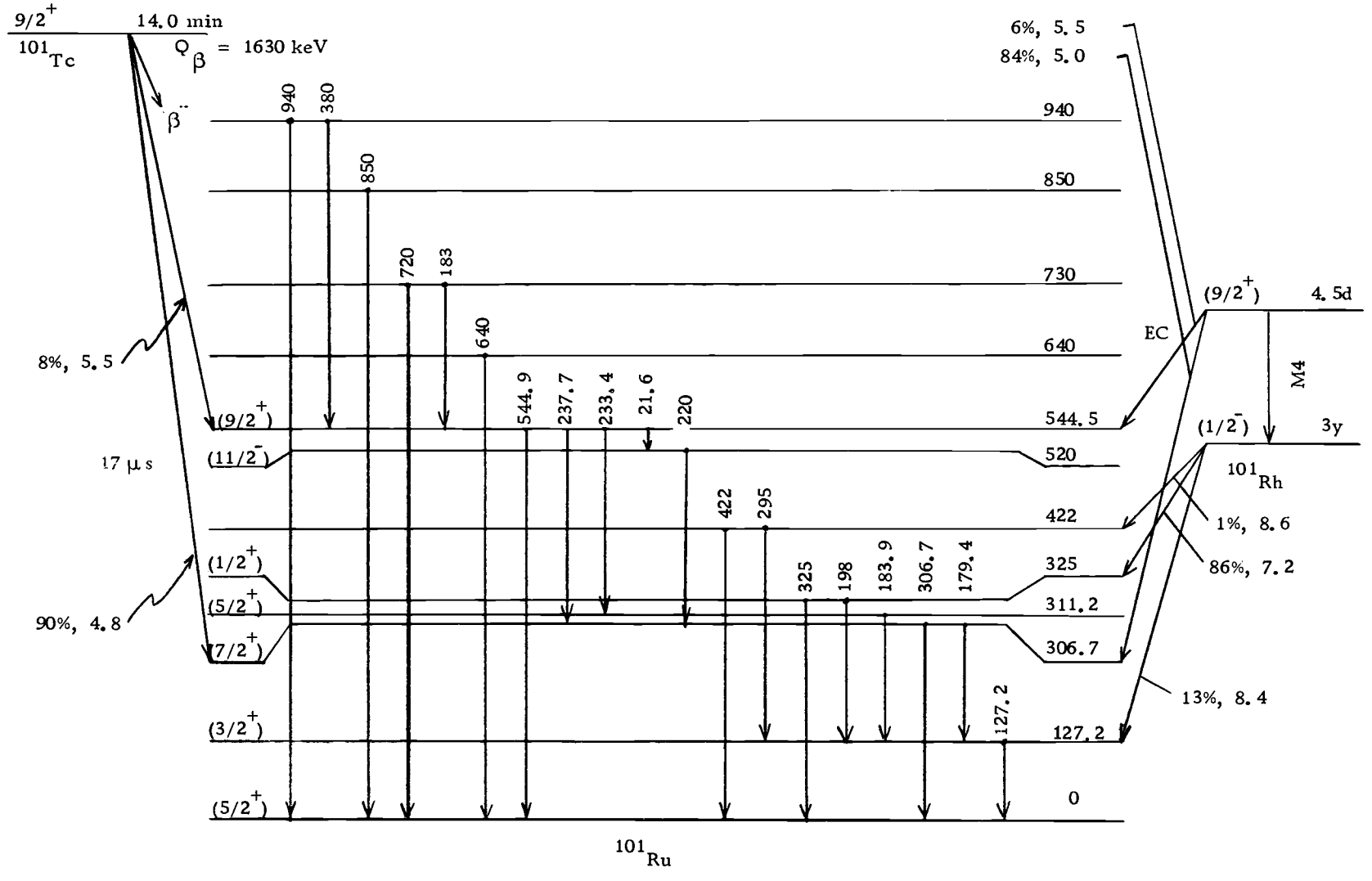

Figure 4. Level scheme of ^{101}Ru , adopted from Lederer et al. (53).

excitation studies of ^{101}Ru nuclei by (α, α') reactions were first performed by Temmer and Heydenburg (88), using scintillation detectors, and recently by Kistner and Schwarzschild (49) utilizing Ge(Li) detectors. However, some levels of ^{101}Ru above 600 keV reported in Coulomb excitation studies were not observed in the previous investigation of the ^{101}Tc decay and vice versa. Therefore the paramount aim of this investigation has been to emphasize study of levels of ^{101}Ru above 600 keV since information pertaining to those levels is unobtainable from the decay studies of ^{101}Rh nuclei.

During the final phase of this investigation additional information on levels of ^{101}Ru were obtained from ^{100}Mo $(\alpha, 3n)$ reaction studies (54). Information in this unpublished report is generally in good agreement with the present investigation.

Information inferred from the decay studies of ^{101m}Rh and ^{101g}Rh suggested that levels of ^{101}Ru may be partially explained by Nilsson model whereas the results of Coulomb excitation studies favor the "core excitation" model.[2] However, predictions of the two theoretical models are far from agreement with experimental observations. The energy-level diagram for ^{101}Ru predicted by Kisslinger and Sorrensen (47), where the core excitation concept is included in the model, is in rather poor agreement with experimental data. Moreover, the model of Kisslinger and Sorrensen even fails to predict a

[2] Will be discussed in more detail in the Discussion chapter.

5/2 spin assignment for the ground state of ^{101}Ru. Since there is no existing nuclear model that can successfully account for all of the energy levels in odd-A nuclei near A = 100, theoretical interest in this region of mass number has been high, emphasizing on the question of whether their level structures are explainable by the spherical models: the vibrational, core excitation weak-coupling, quasiparticle phonon coupling and extended quasiparticle phonon coupling theories. It therefore seemed evident that additional experimental information on ^{101}Ru might prove useful in answering some of the theoretical difficulties.

In addition, the decay of ^{101}Tc is a part of the most interesting decay chain:

$$^{101}\text{Mo} \xrightarrow{\beta^-} {}^{101}\text{Tc} \xrightarrow{\beta^-} {}^{101}\text{Ru},$$

in which half-lives of parents and daughter nuclei not only are relatively short but also are almost equal, i.e., 14.6 minute (91) and 14.0 minute respectively. This makes a study of nuclear level structure of ^{101}Tc from the 14.6 minute ^{101}Mo decay very difficult if the gamma-ray spectrum of the 14.0 minute ^{101}Tc decay is not well established. It is evident that the results obtained from gamma-ray spectrum of ^{101}Tc will provide a very fruitful information pertaining not only to nuclear levels of ^{101}Ru but also, indirectly, to the level structure of ^{101}Tc as well. Particularly, the ambiguity on the

spin-parity assignments of the first two states of ^{101}Tc may be removed by the study of the selective mode of decay of the ^{101}Tc ground state.

EXPERIMENTAL APPARATUS AND PROCEDURES

A block diagram of the gamma-ray spectrometer system used in this study is shown in Figure 5. Fundamental description of how a gamma spectrum of a radioisotope can be obtained from the system is the following: photons striking the detector interact by one of the three processes by which photons interact with matter (i. e. Compton, photoelectric or pair production) giving kinetic energy to an electron which then loses it in collision with shell electrons in the germanium crystal lattice. A trail of electron-hole pairs is produced in the intrinsic region of the germanium crystal. These charged carriers are swept out by the applied electric field providing a charge pulse proportional to the energy lost in the detector by the photon. The pulse is then amplified and shaped by associated electronics prior to the final stage of the system, and an output pulse is created whose amplitude is proportional to the energy absorbed in the detector. The multichannel analyzer, the final component of the system, then sorts the pulse according to its pulse height voltage into one of its few thousands channels. The analyzer output which typically indicates the number of pulses (counts) in each channel represents the gamma energy spectrum of the incident photons.

Each component of the system will be described in detail.

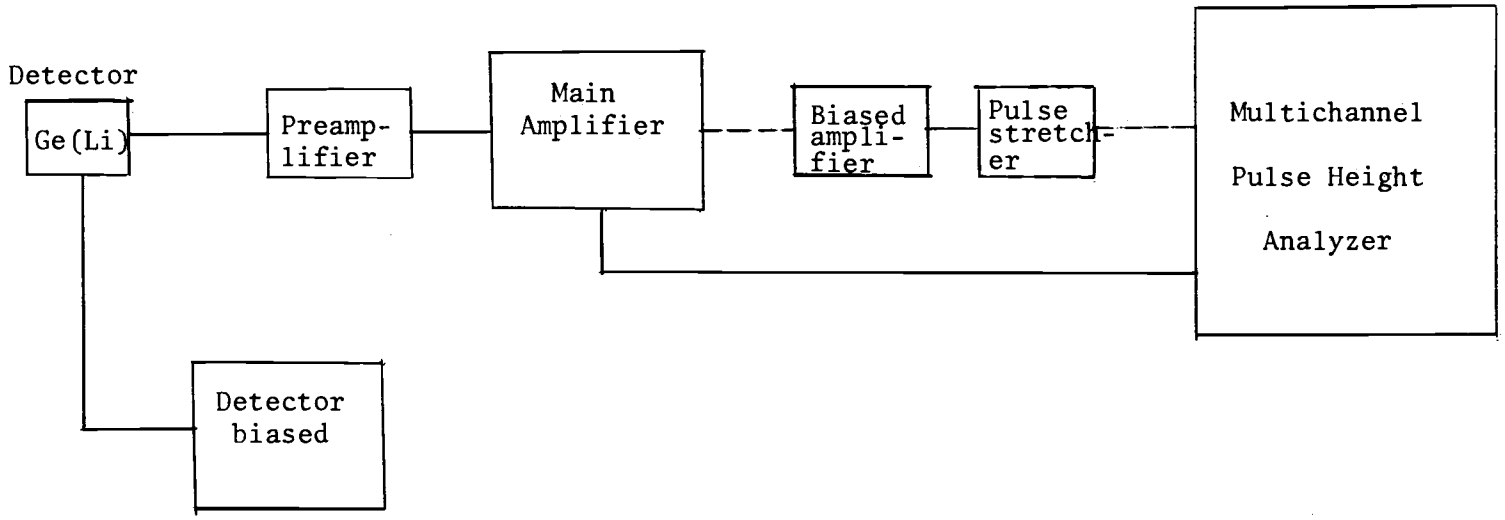

Figure 5. Block diagram of a gamma-ray spectrometer

Detector

Detector is the heart of the gamma-ray detection system and has a great impact on the performance of the system. The Ge(Li) detector, a p-i-n device, is typically constructed from a pure, single crystal of p-type germanium doped with gallium or boron. Many recipes for the Ge(Li) detector fabrication have been described in literature (55, 56, 57, 61, 87). Lithium which acts as an electron donor in germanium is diffused into the crystal, providing an excess number of donors and making germanium n-type. A p-n junction occurs at a point where the numbers of donors and acceptors are equal. Since lithium is a very light ion of high mobility and has a high diffusion coefficient, the drifting process is achieved by an applied bias voltage which creates an electrically neutral region known as intrinsic or compensated region between the n- and the p-type. In such a region collection of free charge carriers is allowed. The drifting process can be terminated when the desired drift depth is attained and the p-i-n device is completed with the undrifted portion of the germanium serving as the p-type region. However, to maintain the p-i-n structure, the Ge(Li) detector must be kept at liquid nitrogen temperature ($77^{o}K$) or colder due to the narrow band gap of germanium and the extreme mobility of lithium ions. A schematic diagram of a planar type Ge(Li) detector adapted from Camp (15) is shown in Figure 6.

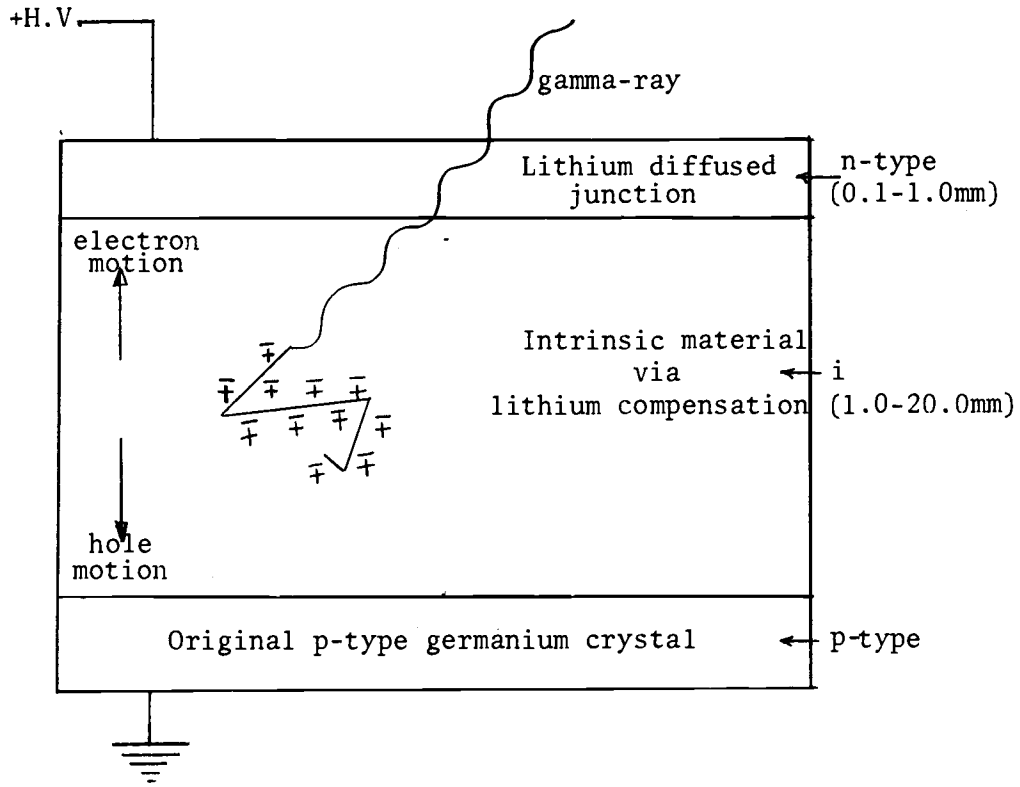

Figure 6. A schematic diagram of a planar-type lithium-drifted germanium detector.

There are three major types of detectors available today. They are planar detector, the true coaxial detector and the five-sided coaxial detector. The planar detector usually consists of a rectangular or circular cross section germanium crystal, the top and bottom being the n- and p-type junctions. For the true coaxial detector, lithium is diffused around the perimeter of a cylindrical ingot and lithium compensation is accomplished by drifting radially toward contacts placed at the center of both ends of the cylinder. But, for the five-sided coaxial detector the geometry of the germanium ingot is either a circular or trapezoidal in shape. Lithium is applied over both the sides and one of the ends. In this case, lithium compensation is achieved by drifting both radially and axially towards a contact place at the center of the remaining open end. If the closed end is mounted toward the source, the five-sided coaxial detector will yield the largest gamma ray full energy peak efficiency per c. c. of active detector volume of any detector shape.

The basic limitation of the energy resolution of a Ge(Li) detector (leaving preamplifier noise and other effects aside) is the statistical fluctuation in the number of electron-hole pairs created for a given photon energy (37). This limit involves the "Fano factor"(29). Consider a gamma ray whose energy E is absorbed completely within the compensated region of a Ge(Li) detector. This amount of energy is used in both the electron-hole pair formation and thermal heating of

the crystal lattice processes (lattice phonons creation). The Fano factor (F) is defined as the ratio of the variance (σ^2) to the number of ion pairs produced (N). If the incident photon energy is E and the energy required for one electron-hole pair is ϵ, then

$$N = E/\epsilon \quad \text{and} \quad F = \frac{\sigma^2}{N} = \frac{\sigma^2}{E/\epsilon} \tag{2.1}$$

The sharing of energy between thermal heating and ionization process is essentially statistical. The statistical fluctuation would not occur at all if all of energy is converted into ionization, hence F = 0. On the other hand, if all of energy is used in the heating process, Poisson statistics would be expected to hold and the variance would be equal to the number of electron-hole pairs, thus F = 1. Nonetheless these two extremes are not the case for Ge(Li) detector. Fano factor value of 0.15 has been reported by Heath et al. (40) and Mann et al. (58). The most recent observed value of the Fano factor in Ge(Li) detector is $F < 0.08$ (74).

To obtain the ultimate resolution in keV, the following formula is used.

$$\Delta E = 2.355 \sqrt{\epsilon E F} \tag{2.2}$$

where ΔE is the full width of the energy peak at half maximum expressed in kiloelectron volts.

For Ge(Li) detector at $77^{o}K$, $\epsilon = (2.98 \pm 0.01) \times 10^{-3}$ keV/ion

pair (1) then ΔE for photon of energy E(keV) becomes

$$\Delta E = 0.1286 \sqrt{EF} \quad . \tag{2.3}$$

If $F = 0.15$ and $E = 100$ keV, we would obtain $\Delta E = 0.50$ keV. However, the contribution from the amplifier noise is generally of the same order of magnitude as the statistical fluctuation due to the basic charge production mechanism. Estimation of ΔE when noise contribution is taken into account will be discussed in connection with the preamplifier.

A detector performance parameter which is the most single important indication of how well a detector will show the presence of gamma rays is known as the "peak to Compton ratio". It is defined as the ratio of the height of the full energy peaks of the incident gamma rays to the height of its mean Compton distribution. The better the detector resolution and the deeper the depletion depth, the larger this figure of merit will be and the more probable it is that weak peaks, normally appearing as a small bump riding on a background of Compton distribtuions of higher energy gamma rays will be observed. This ratio is generally quoted for the standard 1.333 MeV gamma rays of ^{60}Co. As the gamma ray energy increases, this ratio decreases. The ratio depends on the detector energy resolution as well as the detector configuration, primarily the depletion depth. The highest peak to Compton ratio for the Ge(Li) detector presently available is 20/1 for

1. 333 MeV gamma ray. However, a peak to Compton ratio as high as 100/1 is obtained from the Compton suppression system utilizing a Ge(Li) detector (15). In this respect, Compton suppression system has a great superiority in the investigation of a relatively weak peak, particularly those located in the proximity of a prominent peak.

In the beginning of this study a planar type Ge(Li) detector fabricated by the Lawrence Radiation Laboratory was used. It has one cm^2 active area and depletion depth of six mm. Detail information regarding detector assembly has been described elsewhere (92). The resolution of the detector system was typically 3. 0 keV for the 122 keV gamma ray of ^{57}Co and 4. 0 keV for the 1333 keV ^{60}Co gamma ray. Its peak to Compton ratio at 1333 keV was about 4/1. A ten liter dewar of an overhead "chicken-feeder" type is used for supplying liquid nitrogen to the backing plate of the germanium crystal. A Varian Associated eight liter/sec. VacIon pump maintained a pressure of about 5×10^{-7} Torr, in order to avoid condensation on the cold detector. A 510 volt reverse bias was applied to the detector by a RIDL Model 40-14 Power Supply.

The Ge(Li) detector that has taken a major role in this investigation is of trapezoidal type which manufactured by the Nuclear Diodes Inc. It has an active volume of 25 c. c. with 25 mm depletion depth. The energy resolution of the detector system was typically 2. 0 keV for the 122 keV gamma transition of ^{57}Co and 3. 0 keV for the

1333 keV gamma transition of ^{60}Co. The detector capacitance is 11 picofarads and its forward resistance at liquid nitrogen temperature is 14 Kohms. Its peak to Compton ratio when tested at the factory was 18/1. When it is used with the system employed in this study, this figure of merit is 14/1. Its efficiency relative to 3"x3" NaI(Tℓ) crystal at 25 cm source (^{60}Co) - to - detector distance is stated to be 3%. It is mounted so that the n-layer is facing the window which is an aluminum of 0.5 mm thickness, and the crystal is at 16mm away from the window. The schematic representation of its dimensions and "p"-core location is shown in Figure 7. Liquid nitrogen is supplied from a 30 liter dewar. A negative 2200 volt detector biased supply was furnished by a dc power supply of a Berkeley Desimal Scaler Model 2001 which has been modified for negative high voltage power supply. In addition, because of high background in the counting room, a collimator lead shielding unit of about 3" thick and 12 $\frac{1}{2}$" long with 6" inner diameter was used to reduce the background counting rate by a factor of about five.

Since the most distinctive feature of the gamma-ray spectrometer system that make this study a highly successful one is the superiority of the detectors resolution, therefore it would be appropriate to compare gamma spectrum of ^{75}Se taken with the NaI(Tℓ) and the Ge(Li) detector. Figure 8 shows low energy gamma spectrum of ^{75}Se taken with a 3"x3" NaI(Tℓ) whereas Figure 9 shows a gamma

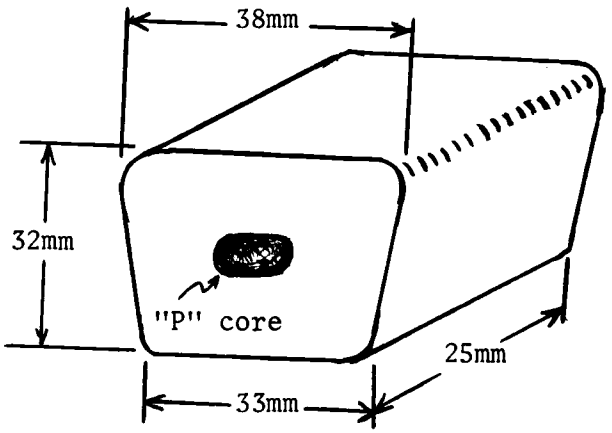

Figure 7. Dimensions of the 25c.c. trapezoidal coaxial Ge(Li) detector.

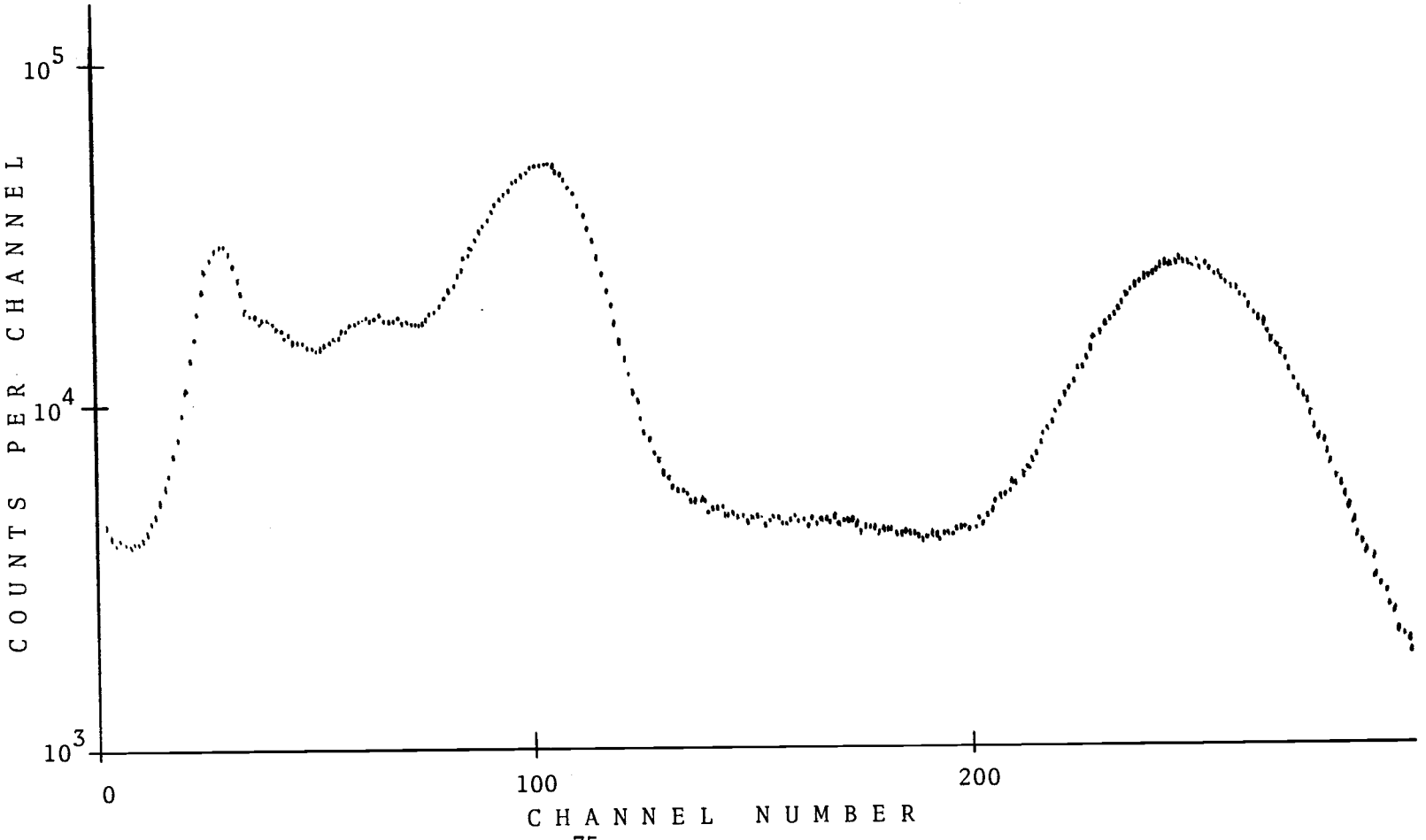

Figure 8. Gamma-ray spectrum of ^{75}Se, taken with a 3"x3" NaI(Tl) detector.

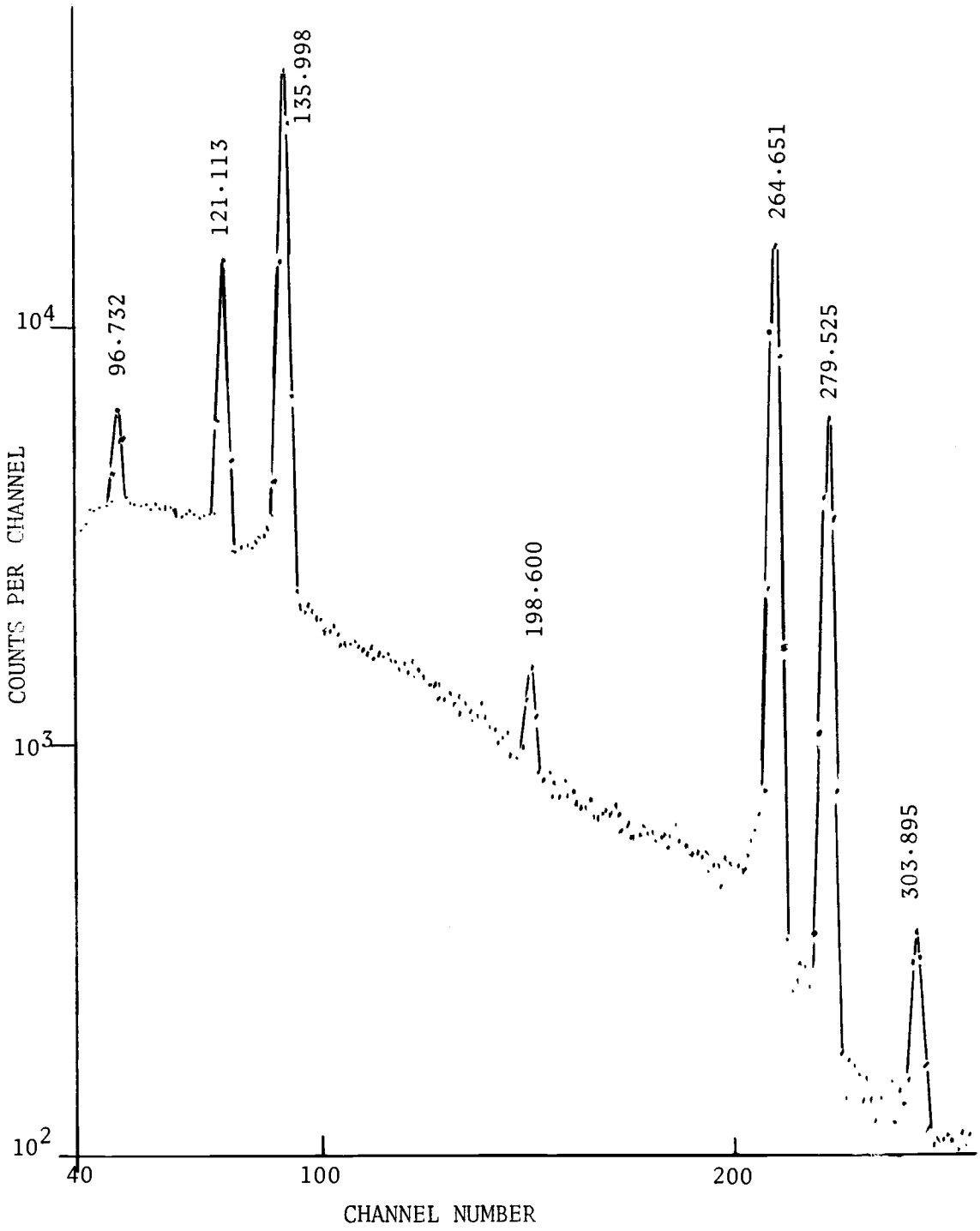

Figure 9. Gamma-ray spectrum of ^{75}se, taken with the 25 c.c. trapezoidal coaxial Ge(Li) detector.

spectrum of the same source but taken with the 25 c. c. trapezoidal Ge(Li) detector.

Preamplifier

The preamplifier used at the beginning of this study was a TMC Model 327A, which is a charge sensitive preamplifier, providing an output signal size independent of the input capacitance. This is a necessary feature since the detector capacitance changes when fluctuations of bias voltage occur (39). Low noise performance is achieved by using a field emission transistor (FET), room temperature operating type, in the input stage. Since the preamplifier noise increases with the input capacitance (76), the FET was mounted directly on the crystal in order to minimize stray capacitance due to the lead-in wire from the detector. Its output pulse has a rise time of about 100 nanoseconds and a decay time of approximately 100 microseconds.

The Nuclear Diodes Preamplifier Model 101A was used with the 25 c. c. Ge(Li) detector. It is integrally mounted on a cryostat without BNC input connector yielding lowest capacitance and most rugged assembly. It has a charge sensitivity of 50 mV/MeV. The output signal of this preamplifier has a rise time of 3.2 microseconds and decay time of 2.0 milliseconds. The integral non-linearity is less than 1%. It is a fast, low noise and uniquely compact preamplifier particularly designed for use with the Ge(Li) detector. The room

temperature FET unit is included to insure low noise performance.

The preamplifier noise figure is normally given by the Equation (15)

$$\Delta W(\text{keV}) = \Delta W_o + mC_D \qquad (2.4)$$

where ΔW_o is the preamp noise figure for zero capacitance (no detector), m is the preamp slope in keV/pf and C_D is the detector capacitance in picofarads.

The Preamplifier Model 101A has $\Delta W_o = 0.7$ keV, $m = 0.018$ keV/pf and the detector capacitance, C_D is given as 11 pf. Therefore, we would expect the preamplifier noise figure of 0.09 keV. The total energy resolution when preamplifier noise is taken into account can be obtained from the relation

$$(\text{FWHM})^2_{\text{total}} = (\Delta E)^2_{\text{Fano factor}} + (\Delta W)^2_{\text{Preamp noise}} . \qquad (2.5)$$

If E is expressed in MeV, ΔW in keV, then the minimum resolution in keV to be expected, from this system is given by

$$(\text{FWHM})^2 = (0.90)^2 + 16.5\,EF . \qquad (2.6)$$

For $F = 0.08$, and $E = 1$ MeV we would obtain the ultimate resolution of 0.97 keV for 1 MeV gamma ray.

Main Amplifier

Two amplifiers were used in this study, the Ortec Model 440 Selectable Active Filter Amplifier and the Ortec Model 435A Active Filter Amplifier. These amplifiers use active filter networks for pulse shaping rather than passive circuits. The Model 440 has a selectable shaping times of 0.25, 0.5, 1, 2, and 4 microseconds, whereas the Model 435A has fixed shaping time of 1.5 microseconds for unipolar and 1.1 microsecond for double clip output pulses. Two main purposes of pulse shaping are preventing pulse overlapping by making the pulse width short with respect to the average spacing of the pulses, and enhancing the signal to noise ratio by removing the relatively wide band width noise components from the signal. It has been shown that a Gaussian shape pulse provides a good signal-to-noise ratio (28). Active network filters resulting in an approximately Gaussian shape output pulse, thus, a good signal-to-noise ratio is produced. In this study a 1.0 microsecond shaping time and unipolar output pulses were selected when the Model 440 was employed, and unipolar output pulses were selected for the Model 435A in order to obtain optimum resolution at typically counting rate (about 200,000 counts per minute).

With the type of RC integration and differentiation used in shaping the pulse, the high resolution offered by the Ge(Li) detector will

decrease as the counting is increased. A technique that allows a substantially high counting rate without deteriorating the detector resolution is known as "pole-zero-cancellation" (11). However, this technique may cause an increase in the low frequency gain of the amplifier, hence microphonics generated in any component in the input circuit of the preamplifier can offset the expected improvement offered by the pole-zero-cancellation technique. Both Model 440 and Model 435A have pole-zero-cancellation feature. This useful feature helps to eliminate the undershoot that results from differentiation by the first clipping network. This exponential tail of the preamplifier output signal usually occurs in an amplifier where pole-zero-cancellation network was not provided. Under overload conditions this undershoot is often large enough to saturate the amplifier creating an undesirable excessive dead time. In a pole-zero-cancellation network, a dc path is provided across the capacitor in the clipping network. In effect, it adds an alternated replica of the preamplifier pulse to just cancel the negative undershoot of the differentiating network so the pulse undershoot is eliminated.

Biased Amplifier

The biased amplifier, also referred to as a threshold amplifier or a window amplifier, permits expansion of any portion of a gamma-ray spectrum over the entire range of the pulse height analyzer. For

example, suppose that a particular portion of the spectrum is extremely complex or of special interest. This portion can be expanded over the entire range of the analyzer with the aid of a threshold discriminator, by which only those pulse amplitudes above the minimum pulse height of the region of interest are allowed to amplify. It does this by providing a continuously adjustable dc biased voltage to reduce the amplitude of all the input pulses, in order that the pulses above the bias level can be amplified without saturating the amplifier.

An Ortec Model 408 biased amplifier was used throughout this study. The Model 408 has a base line restoration network which forces the signal to return to the base line immediately after each pulse. This feature helps to reduce base line shift when counting rates are high. This biased amplifier was used for expanding the complex portion of the spectrum particularly the intermediate energy gamma spectrum of ^{101}Tc. When the biased amplifier was used, an Ortec Model 411 Pulse Stretcher was employed to stretch the peak voltage of all pulses to a minimum pulse width because not all of output pulses from Model 408 Biased Amplifier are wide enough to allow accurate amplitude analysis of the signal by the analyzer. However, when the Northern Scientific multichannel analyzer was used in the system, the biased amplifier component was no longer necessary.

Multichannel Pulse Height Analyzer

Two multichannel analyzers were used in this study. A TMC Model 404 400 - channel analyzer having integral linearity of 0.5% of full scale over the top 97% of the scale was used in the early phase of this investigation. A Dual Parameter 2048 Channel Pulse Height Analyzer Northern Scientific Model NS630 had taken major role in data collection later in the experiment.

Coincidence studies using a 3"x5" NaI(Tℓ) detector as a gate and the 25 c. c. Ge(Li) for observing the spectrum were carried out with the aid of the Two Parameter Coincidence Adapter Model NS641. However, the results obtained failed to prove significant as to levels of ^{101}Ru. Coincidence studies of this decay are made difficult because of the shortness of the parent half-life, but mainly because of 90.3% of the ^{101}Tc beta rays (with 1.32 MeV energy limit) go to the 306.8 keV level; this superimposes a large bremsstrahlung continuum on the gamma spectra in addition to the large Compton background of the intense 306.8 keV transition. Previous gamma-gamma coincidence studies, utilizing two 3"x3" NaI(Tℓ) detectors and a two parameter 2048 channel pulse height analyzer, of ^{101}Tc decay (19) indicated the 127 keV transition to be in coincidence with all transitions between 127 and 720 keV levels. This is in clear disagreement with the results of ^{101}Rh decay studies (3, 17, 26) where the above experimental difficulties do not exist.

EFFICIENCY CURVE

When incident photons interact with a Ge(Li) detector, the amount of interaction is governed by relative cross sections for three basic processes by which photons interact with matter: the photoelectric effect, Compton scattering and pair production. All of the incident photon energy is transferred to kinetic energy (reduced by the binding energy) of an electron only in the photoelectric effect and, in turn, this energy goes into the formulation of electron-hole pairs in the crystal. In the Compton scattering process part of the incoming photon energy is given to an electron and the remaining energy appears as a scattered photon. This process results in incomplete energy deposition if the scattered photon escapes from the detector. In pair production, increasingly probable above 1022 keV, the electron-positron pair is created in the field of a nucleus and the energy of the incoming photon appears as kinetic energy between the members of the pair (with $2m_o c^2$ rest energy required to form the pair). Since the fate of all positrons is annihilation, as soon as a positron slows down, it is captured by an electron from the crystal and is annihilated. Annihilation at rest creates two 511 keV photons which are emitted in opposit directions. In a small detector these annihilation photons usually escape the detector without further interaction resulting in a "pair peak" 1.022 MeV below the main line which is called "double

escape peak". There is a small probability that only one of the 511 keV gammas will escape, and in this case a "single escape peak" is produced. As an illustration of these processes a gamma-ray spectrum of ^{24}Na taken with the 25 c. c. Ge(Li) detector is shown in Figure 10. This spectrum indicates evidence of the three fundamental modes of energy absorption: The "full energy peak", which is a sum of contributions from photoelectric effect events, from totally absorbed multiple Compton scattered events and totally absorbed pair production events, at 2754 keV, the "single-escape" peak at 2243 keV, the "double-escape" peak at 1732 keV and the intense Compton distribution beginning at ~ 2400 keV and extending to low energies.

The energy dependence of the absorption cross section for the three interactions in germanium is shown in Figure 11. These data were taken from Chapman (16). It is evident that the photoelectric effect is predominate below 250 keV and the cross section of this effect decreases roughly four orders of magnitude from 100 keV to 10 MeV. In contrast, the Compton cross section decreases only a little over a factor of ten in the same range of energy.

The immediate implication of the steep slope of the photoelectric effect absorption cross section curve is that a high-energy gamma-ray and a low energy gamma-ray with equal intensity will produce differing numbers of photoelectric events within the detector resulting in a great difference in areas under the peaks. In order to

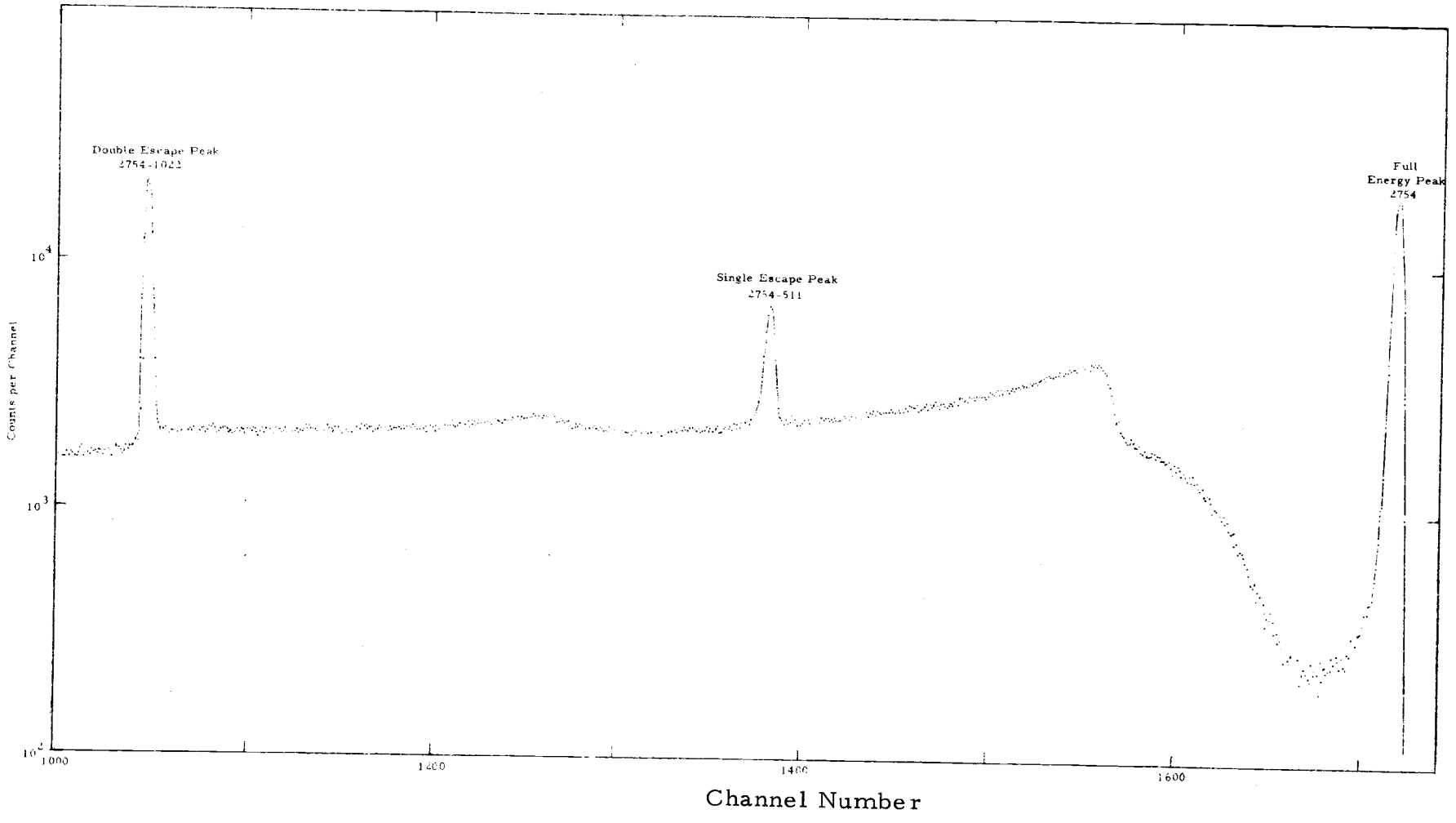

Figure 10. Gamma-ray spectrum of ^{24}Na.

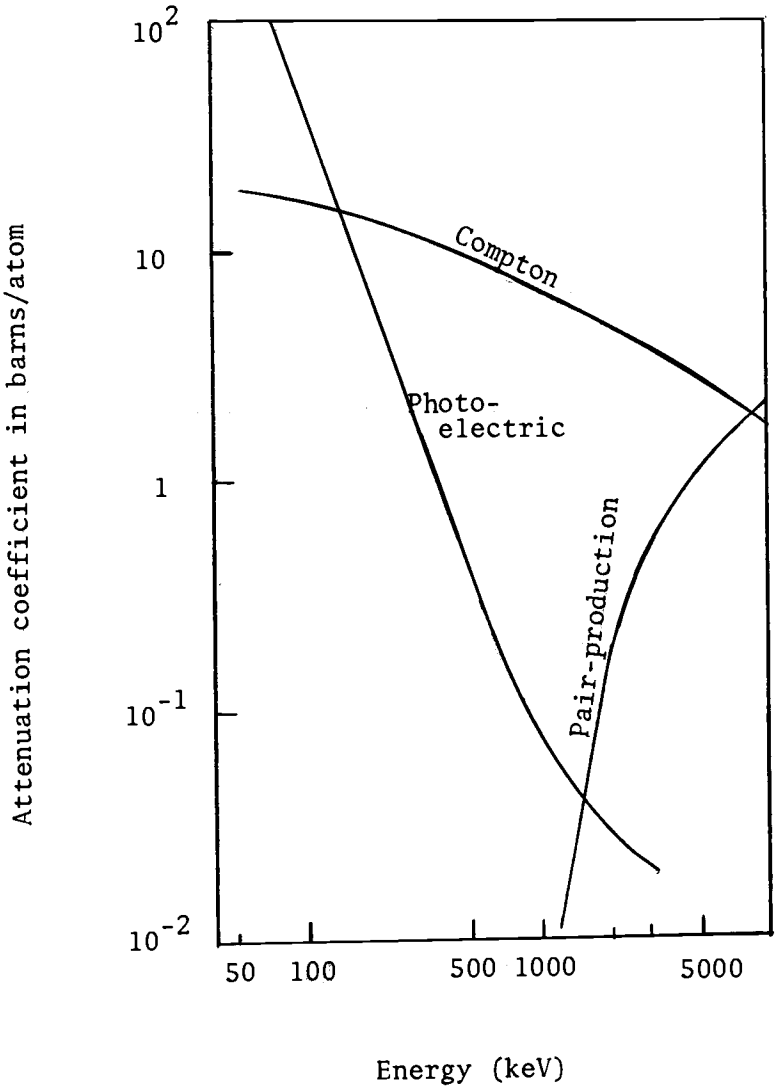

Figure 11. Photoelectric, Compton, and pair-production attenuation coefficients as a function of energy for germanium.

compensate for the energy dependence of the detector efficiency which is defined as the ratio of the number of counts in the full-energy peak to the number of gamma-rays emitted from the source, it is necessary to establish a "relative efficiency curve".

Accurate measurement of gamma ray intensities is very important because it provides important information as to nuclear structure studies, and photon intensities are often sensitive indicators of the validity of nuclear models. In addition, accurate photon intensities incorporated with precise energy data make a construction of a consistent decay scheme possible without relying on coincidence studies. However, the accuracy of photon intensities is limited by the accuracy of the efficiency curve. Therefore, the relative efficiency curve is very important as far as the precision measurement of relative photon intensities is concerned.

Due to the increasing usage of Ge(Li) detectors, a great deal of effort both experimental and theoretical, has recently gone into quantitative analysis of detector efficiencies. Hotz et al. (42) calculated the total counting efficiency curves for various sizes of rectangular Ge(Li) detector. Freeman and Jenkins (33) give the relative full energy peak efficiency, ϵ, as a function of the gamma-ray energy, E, by the expression

$$\epsilon \alpha \left[1 - e^{-\tau x} + A\sigma e^{-BE}\right] \qquad (3.1)$$

where τ and σ are the photoelectric and Compton absorption coefficients of germanium and x is the detector thickness. A and B are empirical constants. Tokcan and Cothern (89) showed that Equation (3.1) was in good agreement (to within 3%) with experimental measurements for a photon energy range of 200 keV to 1500 keV. An empirical method for determining the relative efficiency of a Ge(Li) gamma-ray detector was also simultaneously developed by Kane and Mariscotti (45). After the usage of large Ge(Li) detectors with differing configurations and volumes had become wide spread, Paradellis and Hontzeas (73) established a semi-empirical efficiency equation for Ge(Li) detectors having different active volumes, independent of detector configurations. The relative efficiency, ϵ, of a Ge(Li) detector having active volume, V, for photon energy, E, in a range of 200 to 1500 keV, may be calculated from the following equation

$$\epsilon = k[1 - e^{-\tau V^{1/3}} + 0.012 V\sigma e^{-0.8E}] \qquad (3.2)$$

where τ and σ retain their meaning in Equation (3.1) and k is a constant relating the absolute to the relative efficiency. However, Equation (3.2) must be tested with sufficient number of detectors of differing volumes and configurations before it can be accepted. Since the absolute detector efficiency (to be discussed in more detail later) is a function of source-to-detector distance, thus k should depend on source-to-detector distance as well as gamma-ray energy rather

than being a constant.

Along with the semi-empirical method of the detector efficiency calculation, the Monte Carlo method was first developed by Faria and Levesque (30) for the Ge(Li) detectors having different active areas and different depletion depths in a range of photon energy from 100 keV to 1.5 MeV. But their findings have limited application because of the parallel photon beam assumption. The most recent Monte Carlo calculation for both coaxial and planar type detectors at ten cm source-to-detector distance was carried out by Aubin et al. (4), for photon energies from 100 keV up to 4000 keV to within a 1-3% accuracy. This makes feasible an analysis of gamma-ray energies and intensities simultaneously by a computer. Nevertheless, there are reasons to believe that in a quantitative analysis of gamma ray relative intensities, a calculated efficiency curve should not be used. One of the reasons is that the number of totally absorbed, multiply scattered events is difficult to calculate even with excellent computer codes in which a Monte Carlo program is included. In addition, the amount of single and double escape peak absorption as well as energy dependence bremsstrahlung loses which predominate at high energy (30), is difficult to compute even if the detector configuration and active volume are accurately known. The other reason is that the efficiency curves of two detectors whose external measurable parameters are all identical may not even be similar.

Relative efficiency curves used in this study were constructed following the "pair point" method described by Donnelly et al. (23). The relative efficiency curve for the 1.2 c. c. planar detector was well established by Donald A. Walker (92). Some 44 data points from seven calibrating sources were weighted by a least squares fit in determining the curve. The accuracy of the curve is approximately 10%. For the 25 c. c. trapezoidal coaxial detector, the following calibration sources were used: ^{75}Se, ^{182}Ta, ^{152g}Eu, ^{125}Sb, ^{110m}Ag, ^{226}Ra and ^{24}Na. Energy and relative intensity values used for these well measured standard sources are listed in Table 1. The ratios of well established gamma rays intensities are compared to corresponding ratios of measured peak areas in the spectrum in order to obtain the relative efficiency for each pair point. Since the most prominent peak was typically chosen as a reference peak, the following relation was actually plotted vs. photon energy:

$$\epsilon = A/I \qquad (3.3)$$

where ϵ is the relative efficiency, A is the relative peak area and I is the corresponding relative intensity. This was done for each calibrating source. The resulting relative efficiency curve for each calibration source is placed on a log-log plot. The various plots are graphically superimposed to cover the energy range from 100 keV to 2750 keV and a line of best fit was drawn. A relative efficiency curve

Table 1. Gamma-ray energies and relative intensities for ^{182}Ta, ^{75}Se, ^{152g}Eu, ^{110m}Ag, ^{125}Sb, ^{226}Ra and ^{24}Na.

Isotope	E (kev)	Relative Intensity	Reference
^{182}Ta	100.1	100	a
	113.7	14	
	116.4	3.3	
	152.4	49	
	156.4	20	
	179.4	24	
	198.4	21	
	222.1	52	
	229.3	24	
	264.1	23	
^{75}Se	121.1	27.70 ± 0.5	b
	136.0	95.00 ± 1.80	
	198.6	2.38 ± 0.07	
	264.6	100	
	279.5	42.00 ± 0.80	
	303.8	2.19 ± 0.07	
	400.5	20.4 ± 0.5	
^{152g}Eu	121.78	103.70 ± 3.10	c
	244.66	27.94 ± 0.80	
	344.31	100	
	367.80	3.23 ± 0.12	
	411.13	7.92 ± 0.27	
	443.98	11.75 ± 0.32	
	778.87	48.80 ± 1.10	
	867.33	15.67 ± 0.38	
	964.01	54.53 ± 1.45	
	1085.83 1089.73	46.25 ± 1.10	
	1112.04	51.28 ± 1.40	
	1408.02	80.78 ± 2.10	
^{125}Sb	176.30	22.67 ± 0.63	c
	380.49	5.03 ± 0.21	
	427.90	100	
	463.40	35.11 ± 0.82	
	600.56	60.20 ± 1.40	
	606.68	16.55 ± 0.55	
	635.90	38.80 ± 0.90	
	671.42	6.15 ± 0.22	

Table 1 continued.

Isotope	E (keV)	Relative Intensity	Reference
^{110m}Ag	446.79	3.5 ± 0.2	d
	620.30	2.9 ± 0.2	
	657.72	100	
	677.59	12.2 ± 0.7	
	686.96	7.4 ± 0.6	
	706.65	17.2 ± 0.7	
	744.24	4.4 ± 0.4	
	763.93	24.0 ± 0.8	
	817.99	7.8 ± 0.3	
	884.65	79.6 ± 2.0	
	937.44	36.5 ± 1.1	
	1384.23	27.7 ± 0.8	
	1475.71	4.5 ± 0.2	
	1504.95	14.8 ± 0.4	
^{226}Ra	609.4	42.8 ± 4.0	e
	1120.4	15.0 ± 1.5	
	1238.2	6.1 ± 0.6	
	1764.6	16.7 ± 1.6	
	2204.3	5.3 ± 0.5	
^{24}Na	1368.5	100	f
	2753.9	100	

a = reference 94, b = reference 72, c = reference 5, d = reference 12, e = reference 52, f = reference 53.

for the 25 c. c. Ge(Li) detector using this process is shown in Figure 12. At least four measurements were performed for each standard source in determining the area ratios. Source to detector distances were varied from one to sixteen centimeters. It was found that relative areas under peaks are independent of source-to-detector distance within the experimental errors of peak area determinations. The accuracy of the curve is estimated to be 6% at $E < 1$ MeV and 10% at $E > 1$MeV. The curve was tested by using it to determine the relative photon intensities of well measured lines in the gamma spectra of ^{99}Mo, ^{46}Sc and ^{207}Bi, and it was found that the relative intensities could be reproduced to within a 10% accuracy.

Another useful quality that may be necessary is the ratio of areas of the full-energy peak to escape peak. This ratio may be used in helping to identify escape peaks or in an unusual situation to estimate the contribution of an escape peak to a full-energy peak in case the two have the same energy. Such an unusual situation occurs in the gamma spectrum of ^{61}Cu (92). Fortunately, all gamma transitions from the ^{101}Tc decay have energy less than the pair production threshold, therefore such an overlap will never occur in this spectrum.

There are two types of information concerning the detector efficiency usually provided by the manufacturer: the absolute intrinsic full-energy peak efficiency and the efficiency relative to a standard NaI. The absolute intrinsic full-energy peak efficiency is defined

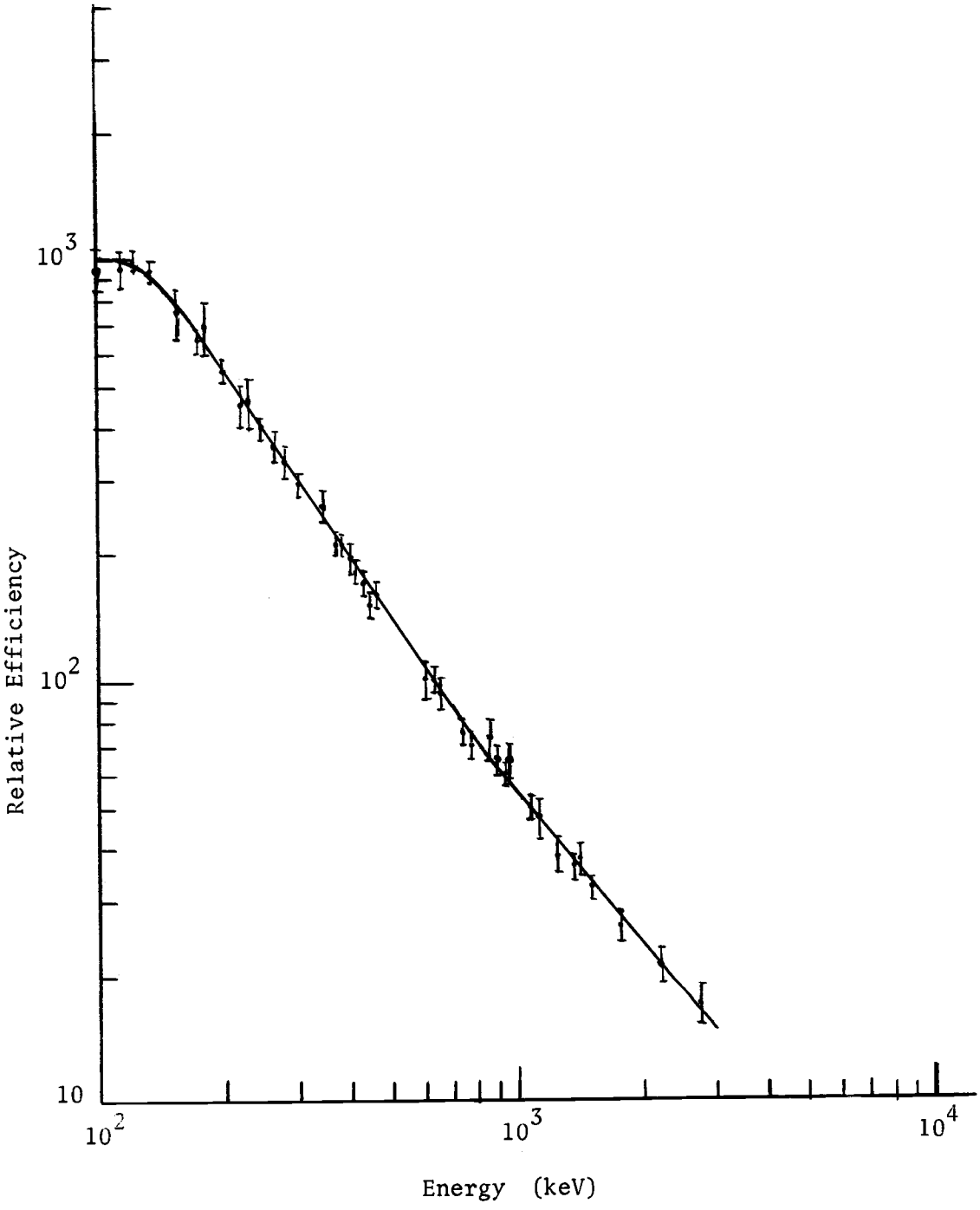

Figure 12. Relative efficiency vs. photon energy for the 25 c.c. Ge(Li) trapezoidal coaxial detector.

as that fraction of events collected in the full energy peak relative to the total number of events which pass through any portion of the detector whether they interact or not. The area of the full-energy peak of a gamma ray of energy E in number of counts N is given by

$$N = S \cdot \Delta\Omega \cdot \Delta t \cdot \epsilon \tag{3.4}$$

where S is the number of gamma ray emitted per second into the solid angle $\Delta\Omega$, Δt is the counting time (sec) and ϵ is the detector absolute efficiency. Therefore ϵ may be directly determined from Equation (3.4). However, in determining ϵ, a set of calibration standards is needed. The efficiency relative to a NaI(Tℓ) detector is easier to determine since all that is needed are a number of sources not necessarily calibrated. Then for equal counting time one obtains from Equation (3.4)

$$\epsilon_{Ge(Li)} = \left(\frac{N}{\Delta\Omega}\right)_{Ge(Li)} \cdot \left(\frac{\Delta\Omega}{N}\right)_{NaI} \cdot \epsilon_{NaI} \tag{3.5}$$

The product $(\frac{\Delta\Omega}{N})\cdot\epsilon$ of NaI may be obtained from published curves in literature. The efficiency of a Ge(Li) detector relative to that of a NaI detector increases as the source-to-detector distance decreases. This occurs because the edge effects are more serious for the larger NaI detector than for the Ge(Li) detector. The amount of increase is a strong function of the detector configuration. The percentage

increase is smaller for the truely coaxial geometry and largest for the trapezoidal (or five sided) configuration. Therefore, the trapezoidal detector is suitable for detecting low intensity gamma lines whereas source-to-detector distance can be minimized such as this investigation. It was found that for a five-sided detector whose relative efficiency at 1.33 MeV is 4% at 25 cm distance, can have a relative efficiency in excess of 10% for a 1.5 cm distance (80). For the 25 c.c. trapezoidal Ge(Li) detector used in this investigation, its efficiency relative to the 3"x3" NaI(Tℓ) detector at 1.33 MeV is 3% at 25 cm distance. There is no simple relationship between the absolute efficiency and efficiency relative to NaI detector. In rare cases, Ge(Li) detectors have been observed to undergo abrupt changes in efficiency. Because these cases are very rare, and since so far it has been impossible to pinpoint the exact time of change, until now there have been no explanation for the sudden changes. Therefore the shape of the relative efficiency curve shown in Figure 12 should not be assumed to be invariant but should be checked periodically.

NUCLEAR LEVEL STRUCTURE OF ^{101}Ru

The ^{101}Ru nuclide is composed of 44 protons and 57 neutrons. This isotope is a very promising case for the nuclear structure studies of mass number 101, since levels can be populated either by the beta decay of ^{101}Tc or by the electron capture decay of ^{101m}Rh and ^{101g}Rh isomers.

Significant studies of ^{101}Ru levels from the ^{101}Tc decay in the presemiconductor detectors period are those performed by Rutledge et al. (79), Wiles (91) and O'Kelley et al. (71). However, the most comprehensive work is that of O'Kelley et al., in 1957, where beta-ray spectra having end point energies of 1.32 and 1.07 MeV as well as the gamma-ray spectrum were measured. In addition, beta-gamma and gamma-gamma scintillation coincidence studies were also carried out by this group. Their findings plus information obtaining from the Coulomb excitation (65, 88) and the ^{101}Rh decay studies (31) were incorporated into the level scheme of ^{101}Ru as shown in Figure 13, taken from the Nuclear Data Sheet (93). Many ambiguities occur in the level scheme and it was not at all clear that levels of ^{101}Ru observed in the decay studies were the same as those seen in the Coulomb excitation work. The remaining unsolved problems were beyond the capability of spectrometers available during that time. No further investigation was made until 1965 when extensive investigations

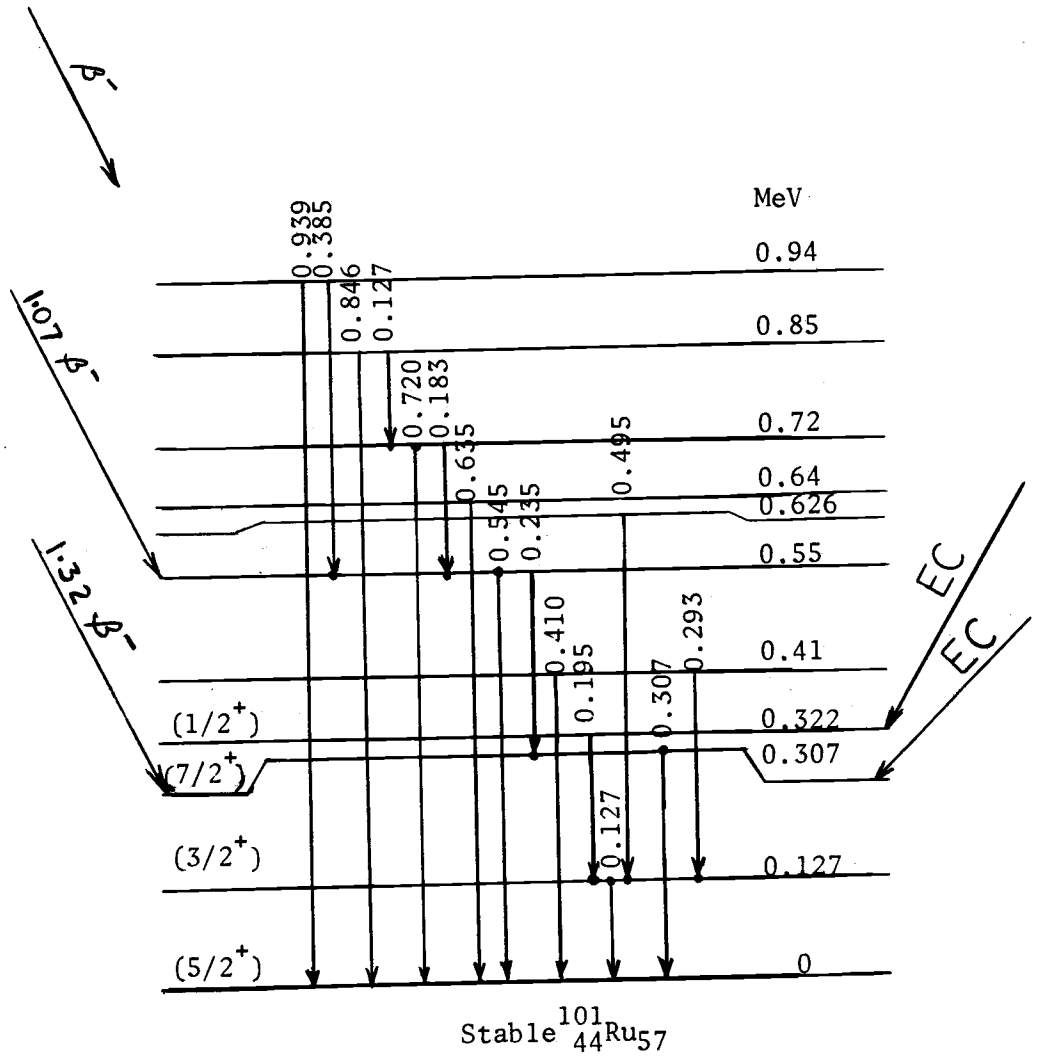

Figure 13. Energy level of ^{101}Ru, taken from the Nuclear Data Sheet (93).

of ^{101}Ru nuclear levels were begun. Scintillation gamma-gamma coincidence studies, using a two parameter 2048 channel pulse height analyzer, of ^{101}Tc decay were made for the first time by Cretu and Funke (19). Many new coincidence relationships between gamma-rays emitted in the ^{101}Tc decay were reported in their study. The first published decay scheme of ^{101}Tc proposed by Cretu and Funke is shown in Figure 3. Dzhelepov et al. (25) reported a plethora of gamma-rays observed in the ^{101m}Rh decay using a conversion electron spectrometer and scintillation spectrometers. But it was not stated in their report whether all the purported transitions had been followed in time to insure that each transition had a 4.5 day half-life. With the aid of a small Ge(Li) detector and magnetic spectrographs Evans and Naumann (26), and Connor (17) reinvestigated the low-lying levels of ^{101}Ru from the electron capture decay of ^{101}Rh isomers. Their successful findings which had little in common with those of Dzhelepov et al. were combined along with partial results of Cretu and Funke in the level scheme of ^{101}Ru compiled by Lederer et al. (53) as shown in Figure 4. It seemed, therefore, that low-lying levels of ^{101}Ru were reasonably well established. In 1966 Aras et al. (2, 3) reinvestigated levels of ^{101}Ru from the radioactive decays of ^{101}Rh as well as ^{101}Tc with the aid of a 0.6 c.c. Ge(Li) detector and a two parameter scintillation coincidence system. Their results on low-lying levels of ^{101}Ru were in good agreement with previous studies (17, 26). However, their

findings on higher levels of ^{101}Ru were rather uncertain due mainly to the low efficiency of their Ge(Li) detector and the shortness in half-life of ^{101}Tc nuclei.

In 1967 studies of ^{101}Ru levels by Coulomb excitation with 4-7 MeV α-particles were carried out by Kistner and Schwarzschild (49) using a Ge(Li) detector and a NaI(Tl)-Ge(Li) coincidence system. These experiments showed that many levels of ^{101}Ru exhibited collective character with enhanced E2 transition probabilities. In addition, two new levels at 616.3 and 623.5 keV which have never been observed in the decay studies were proposed by these authors. However, many ambiguities on levels of ^{101}Ru above 600 keV remained to be resolved by a quantitative study of ^{101}Tc decay.

The Decay of ^{101}Tc

The present investigation of the 14.0 minute ^{101}Tc decay was initiated in 1969. Sources of ^{101}Tc were produced by neutron irradiation of molybdenum trioxide (both natural and enriched in ^{100}Mo) by the reaction and decay:

$$^{100}\text{Mo}(n, \gamma)^{101}\text{Mo} \xrightarrow{14.6 \text{ min}} {}^{101}\text{Tc} \ .$$

Irradiation periods were varied from 5 to 30 minutes at a neutron flux of 1.3×10^{12} n·cm^{-2}·sec^{-1} furnished by the Oregon State University Triga Mark III Reactor. In toto more than 50 irradiations of natural and

isotopically enriched molybdenum targets were made. A rapid, carrier-free separation of TcO_3 from MoO_3 targets was developed which employs the difference in volatility of the two substances. A simple sublimation apparatus is constructed of pyrex glass in the following manner: A vial having a 5 mℓ volume is used to contain the irradiated samples (2-10 gms of oxide). The vial opens to an eight inch length of eight mm ID tubing through a constriction of roughly 0.5mm in diameter. TcO_3 is driven from the sample by careful heating and the radioactive vapor then condenses on the cold walls of the tubing. The tube is separated from the vial by braking it at the constriction and the TcO_3 is washed from the tubing walls with dilute HCl into a sample container for counting.

The only contamination in sources of ^{101}Tc was found to be known lines of ^{99m}Tc with a half-life of 6.04 hours (18). Efficiency of ^{101}Mo - ^{101}Tc separation was ascertained by the absence of the prominent ^{101}Mo lines: 192, 590 and 1012 keV (9). ^{101}Tc samples containing detectable amounts of ^{101}Mo were rejected.

Molybdenum trioxide manufactured by the J. T. Baker Chemical Company in powder form were used as natural targets. The natural abundance and, where applicable, the thermal neutron activation cross sections of the molybdenum isotopes are: ^{92}Mo (15.84%, < 0.006b), ^{94}Mo (9.04%) ^{95}Mo(15.72%, 14b), ^{96}Mo(16.53%, 1b), ^{97}Mo(9.46%, 2b) ^{98}Mo(23.78%, 0.51b), ^{100}Mo(9.63%, 0.2b).

Neutron irradiation of natural molybdenum produces activities of ^{99}Mo(67h), ^{99m}Tc(6.04h), ^{101}Mo(14.6 min) and ^{101}Tc (14.0 min). The chemical purification process was performed when activity of ^{101}Tc attains its maximum value which is about 24 minutes after the end of bombardment (44). Since the gamma-gamma coincidence studies proved unsuccessful, each prominent line of ^{101}Tc has been followed in time to verify that they exhibited a 14 minute half-life and relative intensities of weak lines were compared with the intense ones to insure that they also had the same half-life.

Isotopically enriched molybdenum target material (^{92}Mo, 0.6%; ^{94}Mo, 0.23%; ^{95}Mo, 0.4%; ^{96}Mo, 0.81%; ^{97}Mo, 0.36%; ^{98}Mo, 1.69%; ^{100}Mo, 95.9%) was obtained from the Oak Ridge National Laboratories.

Neutron irradiation of isotopically enriched targets produce mainly ^{101}Mo and ^{101}Tc isotopes plus a small amount of ^{99}Mo activity. In some runs a trace of ^{24}Na was also observed after ^{101}Mo, ^{101}Tc had decayed away. ^{24}Na was believed to be produced from the reaction ^{23}Na(n, γ)^{24}Na because the thermal neutron absorption cross section of ^{23}Na is quite large, 0.40 barn for producing the 20 millisecond isomeric state and 0.13 barn for making the 15.0 hour ground state of ^{24}Na. Therefore the total thermal neutron absorption cross section of ^{23}Na is 0.53 barn in comparison with 0.2 barn for thermal neutron absorption cross section of ^{100}Mo. The ^{23}Na impurity is believed to be in the isotopically enriched targets or in the

target containers.

The decay scheme (53) of every nuclide having a half-life in the range of 10 to 20 minutes was examined for correspondence to lines in the gamma-ray spectrum. Conversely, with the use of a table of gamma-rays listed according to energy (84) in conjunction with the approximate measured half-life of any suspicious lines in the spectrum, it was possible to check the source of impurity lines.

Low energy gamma-ray spectrum of ^{101}Tc taken with the 25 c.c. Ge(Li) detector for gamma-ray energy from 50 to 350 keV is shown in Figure 14. The only unavoidable impurity lines appear in the spectrum are that of ^{99m}Tc (6.04h). The lowest energy line of ^{101}Tc is the 127.2 keV line which depopulates the well known first-excited level of ^{101}Ru. The most prominent line of the spectrum is the 306.8 keV. This transition is so intense the 295 and 311.2 keV lines which unfortunately occur in its proximity cannot be observed in the spectrum shown in Figure 14. However, later measurements performed by Dr. Harry T. Easterday,[3] utilizing a Compton suppression system, confirm the existence of the weak 295 and 311.2 keV transitions. Gamma-ray spectrum of ^{101}Tc in this region taken with the Compton suppression spectrometer is shown in Figure 15. In addition a bremsstrahlung continuum which accompanies the beta feeding of the 306.8 keV level of ^{101}Ru, along with the high Compton background of the

[3] Private communication.

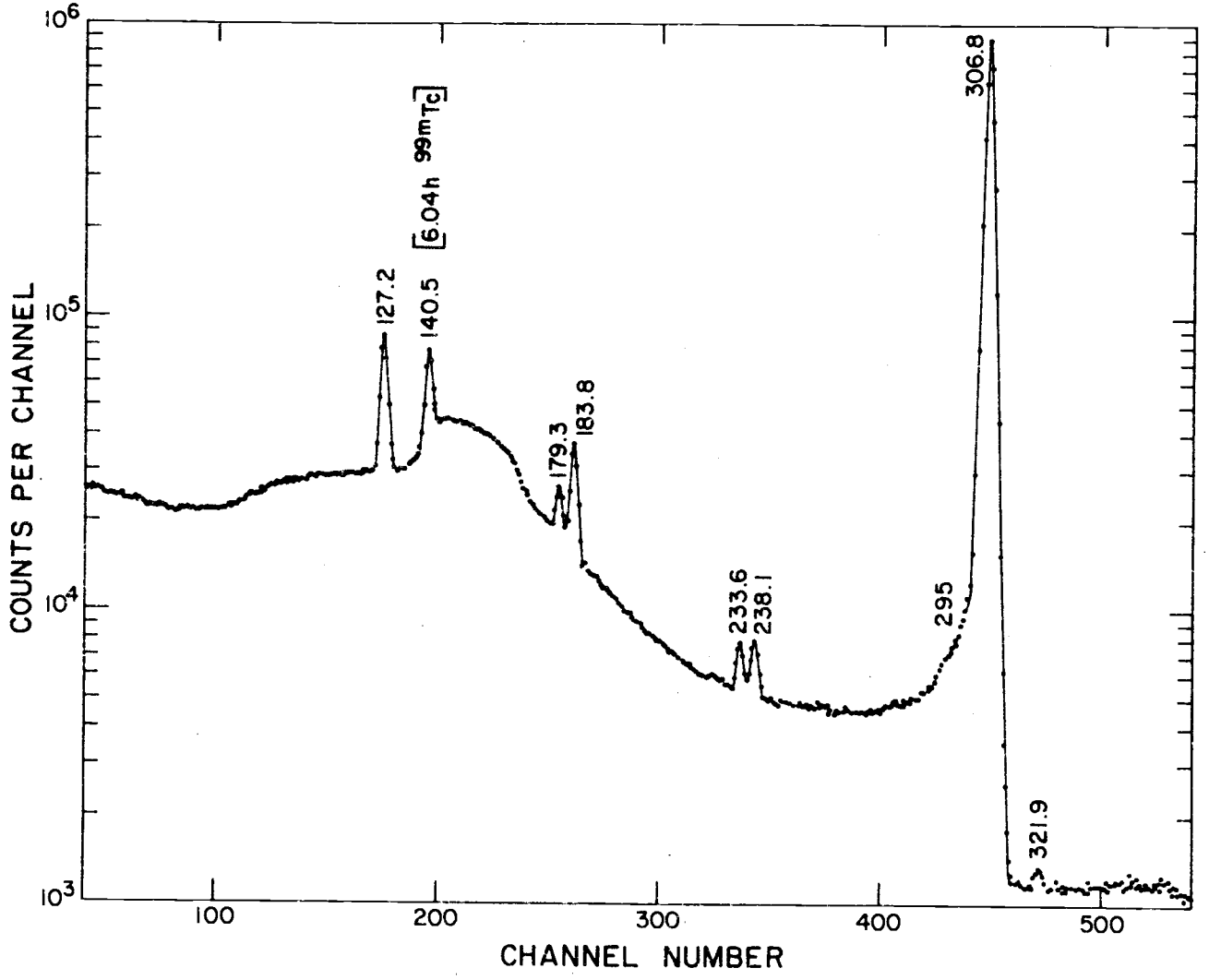

Figure 14. Low-energy gamma ray spectrum of ^{101}Tc.

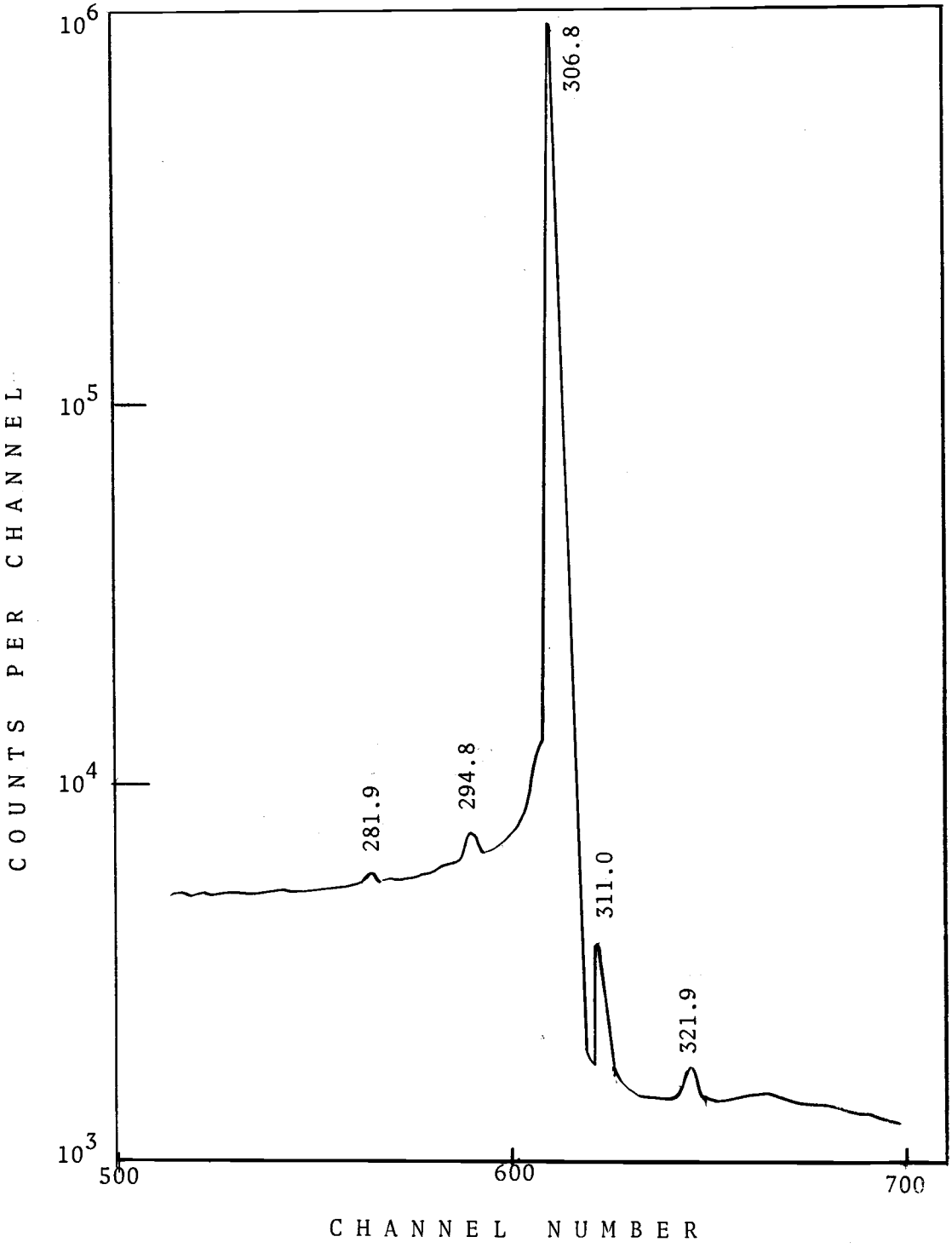

Figure 15. Gamma-ray spectrum of ^{101}Tc in the proximity of the intense 306.8 keV line taken with a Compton suppression spectrometer.

306.8 keV transition, tend to obscure the weak peaks at 110.7, 114.8, and 174.7 keV observed in Coulomb excitation studies (49). The 110.7 and 114.8 keV are expected transitions from the 421.9 keV state to the 311.2 and 306.8 keV levels, and the 174.7 keV line is expected from the de-excitation of the 720.1 keV state to the 544.8 keV level.

Figure 16 shows the gamma-ray spectrum in the region 350 to 650 keV. This and higher energy portions of the spectrum were recorded with a 4.6 mm lead absorber between source and detector to reduce the intensity of the prominent 306.8 keV and 127.2 keV lines and decrease the problems associated with high count rate. The 408 keV line observed in Coulomb excitation studies (49) were not seen in this region of the spectrum. The line at 511 keV is the annihilation gamma ray of an unidentified background. The 617.3 keV line is broader than peaks of comparable energy, indicating two or more gamma transitions of nearly equal energy. Because of the smooth, symmetric appearance of the peak, it is likely to be composed of two gamma rays of approximately equal intensity. According to the energy relationship and intensity balancing, this line is believed to be an admixture of the 616.3 keV - first seen by Kistner and Schwarzschild (49) and the 618 keV - proposed by Aras et al. (2) with roughly equal intensity.

The high energy portion of the gamma-ray spectrum from 650 - 1000 keV is shown in Figure 17. Gamma-ray lines in the neighborhood

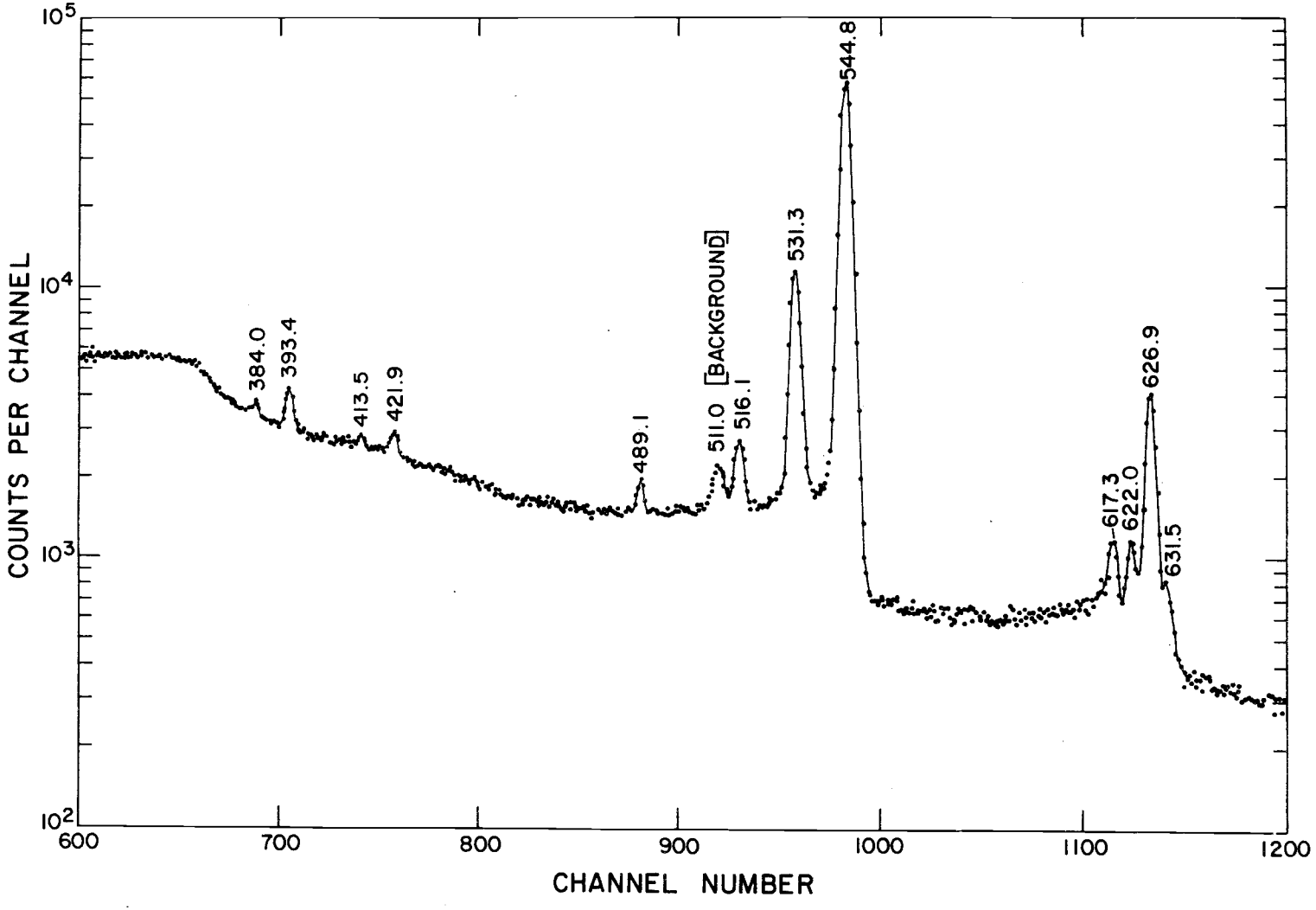

Figure 16. Intermediate-energy gamma spectrum of ^{101}Tc.

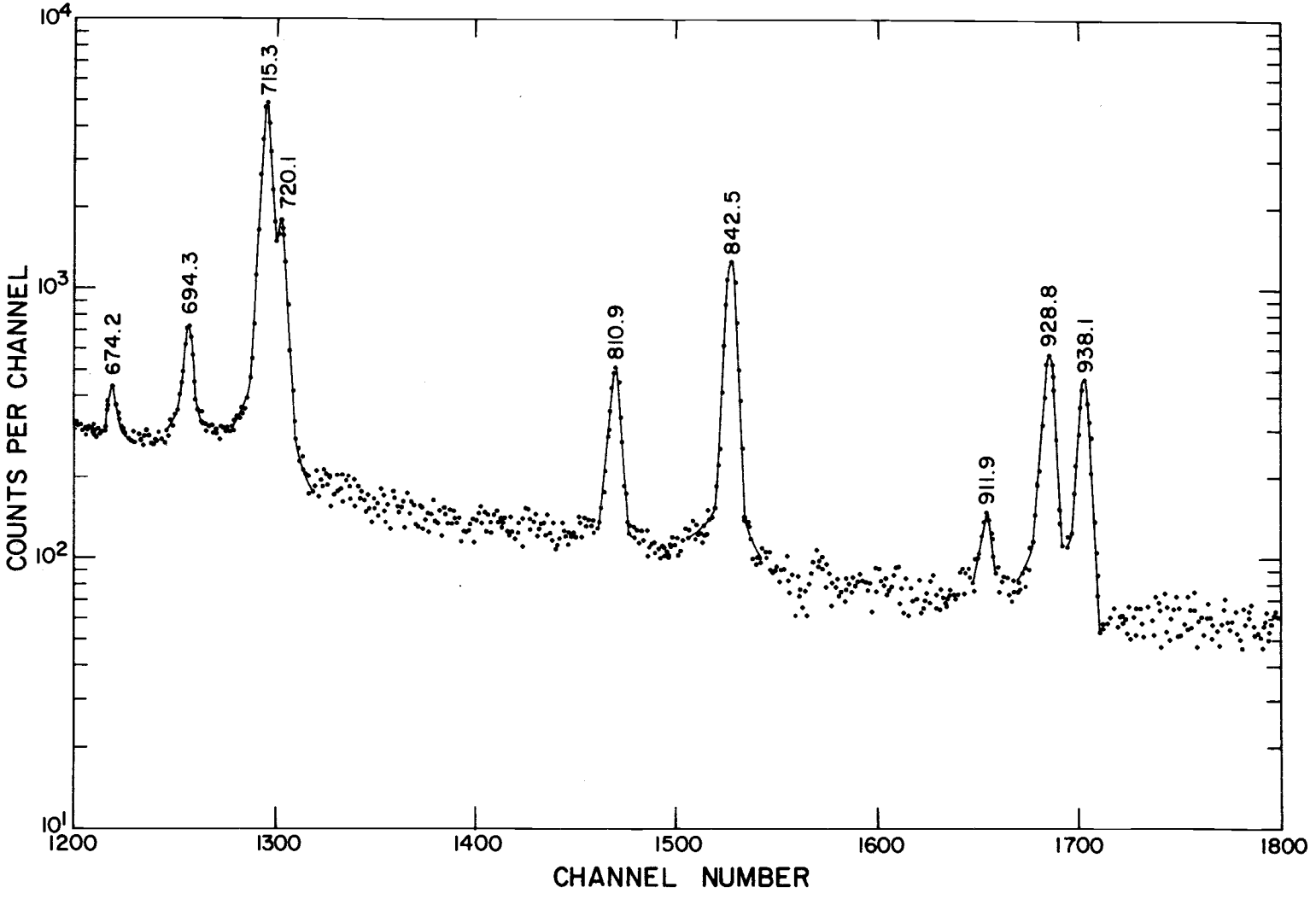

Figure 17. High-energy gamma spectrum of ^{101}Tc.

of 912 keV region were relatively weak and runs as long as four half-life periods were necessary. For accurate relative intensities measurement accumulation of gamma spectrum obtained from several consecutive runs were made.

One possible source of spurious lines is the peaks occurring from the summing of two gamma radiations which have been detected within the resolving time of the detector. The 306.8 keV transition is the potential contributor of any possible sum peaks, therefore, we would expect accidental sum peaks at 424 keV (306.8 + 127.2) and 851.6 keV (306.8 + 544.8). However, no such peaks ever appeared in the spectrum. Moreover, other methods of checking sum peaks were used such as varying the source-to-detector distance and employing lead absorbers. It was found that relative intensities of lines were reduced accordingly which implies that no sum peaks appear in the gamma-ray spectrum of ^{101}Tc.

In deducing the level scheme, reliance was placed on the precision energy measurements as well as intensity balancing. Radioactive sources whose gamma ray energies are accurately known were used to determine energy at a particular amplifier gain setting as a function of channel number for the multichannel pulse height analyzers. The energy of ^{101}Tc lines in a spectrum recorded at the same setting were then calculated with the aid of a least square computer code. Peak positions were determined to within 0.1 channels by finding the

mean position of the three highest points of each line.

Pulse height shift with high count rate was a serious source of systematic error associated with the energy measurements. In order to reduce this effect the calibration sources were recorded roughly at the same count rate as the ^{101}Tc source with the aid of a scaler connected to the output of the main amplifier to serve as a count rate monitor. In this way shifts in the spectrum of as much as 2.0 keV were reduced to < 0.3 keV for the TMC analyzer. An alternative method of eliminating problems relating to base line shift is to record the spectrum calibrating sources simultaneously with the ^{101}Tc source. In this respect only energy of prominent ^{101}Tc lines could be measured. Since the 140.5 keV ^{99m}Tc line is well measured, it therefore serves as a pulse height shift monitor as well as an internal calibrating line.

Nonlinearity in the pulse height versus energy scale introduced by the amplifiers and multichannel analyzer contributed an additional problem associated with the precision energy measurements. With the present day computing facilities, it is possible to calibrate a nonlinearity system to any desired accuracy. However, in practice accurately known calibration lines are available in limited number. Therefore, reliance must be placed on the system linearity. For the TMC multichannel analyzer it was found (6) that by avoiding the first quadrant of its memory, the system nonlinearity could be significantly

reduced. To allow for any remaining departure from linearity of the system, a second order least square program using the Oregon State University CDC 3300 computer was used to fit the calibration points according to the following polynomial equation:

$$E = a + bN + cN^2 \qquad (4.1)$$

where E is the energy, N is the channel number and a, b, c are empirical constants. The least square program was also weighted according to the precision of calibration lines. Typical values of coefficients were b = 1 keV/channel and c = 0.00005 keV/(channel)^2.

To assure that long-term drift will not influence the data chosen for analysis, calibrations were made prior to and subsequent to each run. However, no significant long-term shift was observed during the data collecting periods which typically last one to two hours.

The relative intensities of various gamma rays of ^{101}Tc were determined by using the following equation

$$I_x = I_s \left(\frac{A_x}{A_s}\right) \left(\frac{\epsilon_s}{\epsilon_x}\right) \qquad (4.2)$$

in conjunction with the efficiency curve shown in Figure 12, where I_x, A_x and ϵ_x refer to gamma-ray under investigation and I_s, A_s and ϵ_s refer to the standard line to which all other lines are normalized. In this study the 306.8 keV line since it was the most intense was

chosen to be the reference line, and its peak area and intensity were assigned to be 100. Therefore, Equation (4.2) reduced to the form:

$$I_x = A_x \left(\frac{\epsilon_{306.8}}{\epsilon_x}\right) \qquad (4.3)$$

The quantity in the parenthesis is the correction factor due to the energy dependence of the detector efficiency and can be obtained directly from the relative efficiency curve. The areas of the full-energy peaks in the spectra were determined by subtracting a suitable background and summing the counts remaining in the peak. In those cases in which a lead absorber was used, corrections of intensity data were made using the attenuation coefficients given by White (95).

The energies and intensities of the gamma-rays observed in the decay of ^{101}Tc are listed in Table 2. Uncertainties given for the intensities include errors in measuring area of peaks as well as an estimated error from the efficiency curve. The latter error usually accounted for the greater part of the total error. As mentioned earlier, weak 295 and 311.2 keV transitions expected in the ^{101}Tc decay could not be resolved from the intense 306.8 keV peak, and relative intensities for these lines listed in Table 2 were inferred from intensity balancing. Both transitions have been observed in gamma spectra from ^{101}Rh decay studies (3, 17, 26, 50).

Table 2. Energies, positions, and intensities of gamma rays emitted in the decay of 14.0 minute ^{101}Tc.

Energy (keV)	Relative Intensity	Transition (keV)	
		From	To
127.2 ± 0.1	2.6 ± 0.3	127.2	GRD
179.3 ± 0.2	0.62 ± 0.06	306.8	127.2
183.8 ± 0.2	1.70 ± 0.15	311.2	127.2
233.6 ± 0.2	0.29 ± 0.03	544.8	311.2
238.1 ± 0.2	0.33 ± 0.03	911.9	674.2
		544.8	306.8
295	0.07 a)	421.9	127.2
306.8 ± 0.1	100.	306.8	GRD
311.2	0.01 a)	311.2	GRD
321.9 ± 0.4	0.03 ± 0.01	938.1	616.3
384.0 ± 0.4	0.03 ± 0.01	928.8	544.8
393.4 ± 0.3	0.11 ± 0.02	938.1	544.8
413.5 ± 0.5	<0.01	720.1	306.8
421.9 ± 0.3	0.04 ± 0.01	421.9	GRD
489.1 ± 0.3	0.03 ± 0.01	616.3	127.2
516.1 ± 0.2	0.11 ± 0.02	938.1	421.9
531.3 ± 0.1	1.14 ± 0.07	842.5	311.2
544.8 ± 0.1	6.7 ± 0.6	544.8	GRD
617.3 ± 0.4 b)	0.06 ± 0.01	616.3	GRD
		928.8	311.2
622.0 ± 0.4	0.04 ± 0.01	928.8	306.8
626.5 ± 0.2	0.50 ± 0.08	938.1	311.2
631.5 ± 0.5	0.03	938.1	306.8
674.2 ± 0.4	<0.01	674.2	GRD
694.3 ± 0.2	0.05 ± 0.01	1001.1	306.8
715.3 ± 0.1	0.7 ± 0.1	842.5	127.2
720.1 ± 0.2	0.24 ± 0.06	720.1	GRD
810.9 ± 0.2	0.07 ± 0.02	938.1	127.2
842.5 ± 0.1	0.21 ± 0.04	842.5	GRD
911.9 ± 0.2	0.02 ± 0.01	911.9	GRD
928.8 ± 0.1	0.09 ± 0.01	928.8	GRD
938.1 ± 0.1	0.08 ± 0.01	938.1	GRD

a) Deduced from the intensity balancing

b) Unresolved doublet

The Level Scheme of ^{101}Ru

The proposed level scheme of ^{101}Ru is shown in Figure 18. The decay scheme of ^{101}Tc was established based on the gamma-rays measurements of this study with the aid of well established information obtaining from previous studies of Coulomb excitation (49), ^{101}Rh (3, 17, 26) and ^{100}Mo (α, 3n) reactions (54). The decay scheme of ^{101m}Rh and ^{101g}Rh were adopted from reference 3.

In the decay scheme of ^{101}Tc, (Figure 18a), the β-groups energies were obtained by subtraction of level energies from the Q_β value listed in reference 60. Beta-branching ratios and the total population of the excited states of ^{101}Ru were deduced from the observed γ-ray intensities. The effect of the internal conversion process was not taken into account because the effect is not large and the correction was found to be less than the uncertainty in gamma-rays intensities. Log ft values were calculated utilizing the Moszkowski nomograms (66). The pair of numbers with each gamma transition gives the gamma-ray energy in keV and in parenthesis the relative intensity. The trio of numbers for each beta decay gives the transition energy in MeV, β branching in percent, and log ft value.

Energy levels of ^{101}Ru is deduced in the following way: energy balance relationships are sought which indicate the presence of two or more cascade gamma rays and the corresponding crossover transition.

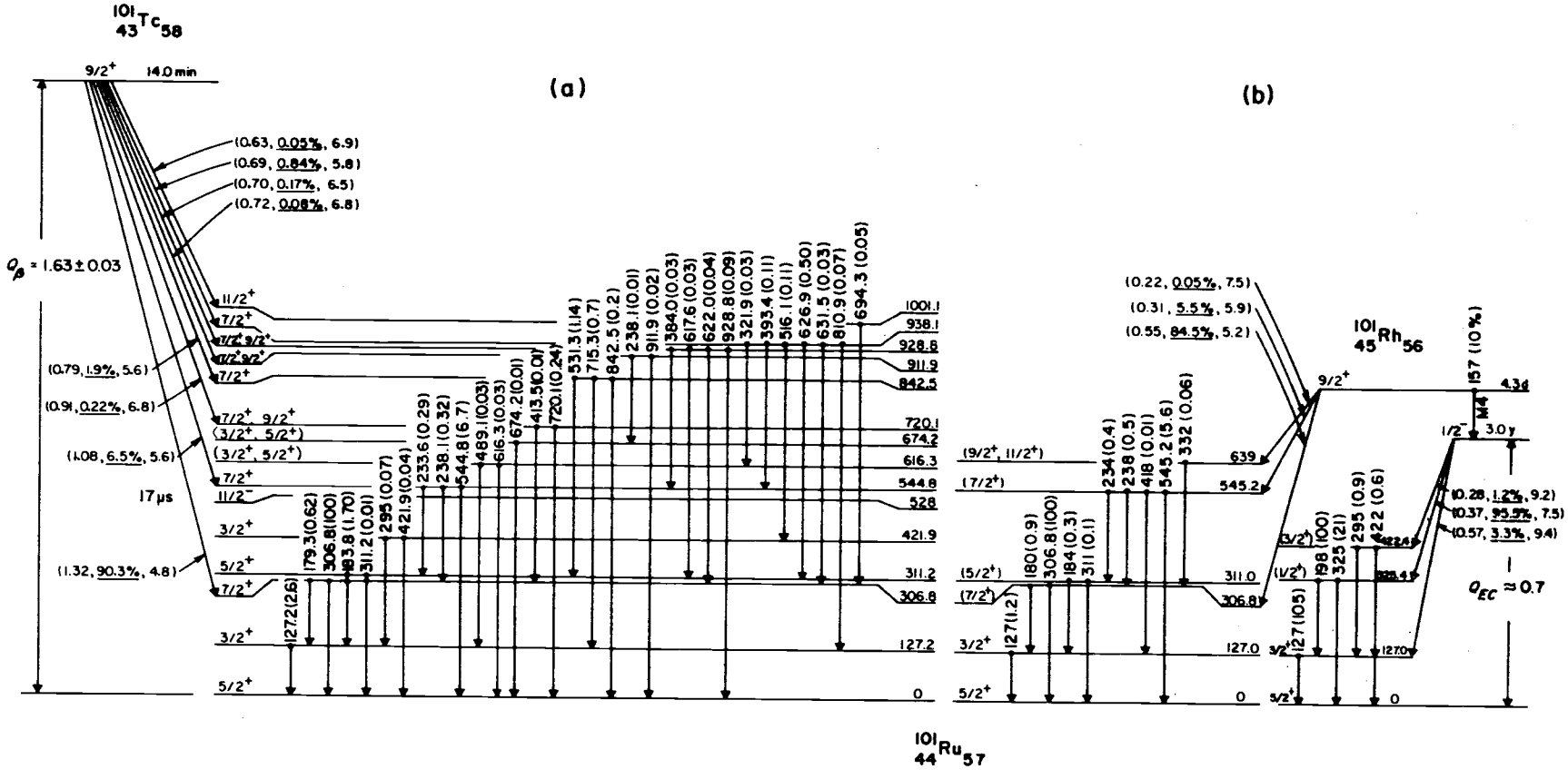

Figure 18. Proposed level scheme of ^{101}Ru.

Energy levels which would accommodate these transitions are then proposed. To distinguish between true and accidental energy relationships, recourse is made to previous well established data obtained from radioactive decay, Coulomb excitation and nuclear reaction studies as well as data from gamma-gamma coincidence investigations.

The following groups of energies have the characteristic that the sum of the first two energies equal the third within the experimental error:

1) 127.2, 179.3, 306.8
2) 127.2, 183.8, 311.2
3) 127.2, 295, 421.9
4) 127.2, 489.1, 616.3
5) 306.8, 238.1, 544.8
6) 306.8, 413.5, 720.1
7) 306.8, 622.0, 928.8
8) 306.8, 631.6, 938.1
9) 311.2, 233.6, 544.8
10) 311.2, 531.3, 842.5
11) 311.2, 617.6, 928.8
12) 311.2, 626.9, 928.1
13) 421.9, 516.1, 938.1
14) 544.8, 384.0, 928.8
15) 544.8, 393.4, 938.1
16) 616.3, 321.9, 938.1
17) 674.2, 238.1, 911.9

From previous extensive studies, ^{101}Ru is well known to have first and second excited states at 127.2 and 306.8 keV. The third excited state at 311.2 keV was established from quantitative studies of ^{101m}Rh decay (3, 17, 26).

The 325.4 and 421.9 keV excited states have been established by ^{101g}Rh electron capture decay (3, 17, 26), by ^{101}Tc β-decay (2),

and Coulomb excitation studies (49).

The isomeric state at 528 keV has been established by the (α, 3n) reaction studies (54). Evans and Naumann (26) proposed this level at 523 keV.

The excited state at 544.8 keV has been well established by ^{101}Tc decay (2, 19, 59, 71), by Coulomb excitation (49), and by ^{101m}Rh decay studies (3, 17, 26). The energy relations 1), 2), 3) and 5) confirm the previous establishment of the low-lying levels of ^{101}Ru at 127.2, 306.8, 311.2, 421.9 and 544.8 keV.

The energy relation 4) suggests a new level at 616.3 keV. Supporting this assignment is the Coulomb excitation studies of Kistner and Schwarzschild (49), who proposed this level for the first time. The energy relation 17) and intensity balancing suggest two new levels at 674.2 and 911.9 keV.

A new level at 938.1 keV is suggested by relation 8), 12), 13), 15) and 16). This level is also accommodate the 321.9 keV transition.

In order to accommodate the 694.3 keV transition a new level at 1001.1 keV is proposed. This proposal is in good agreement with a new level at 1001 keV found in (α, 3n) reaction studies (54).

Spins and Parities of Nuclear Levels in ^{101}Ru

A great deal of previously reported data was available for establishing spins and parities of low-lying levels of ^{101}Ru.

Information pertaining to spin-parity assignments of levels in ^{101}Ru below 545 keV inferred from the present study agrees with that of previous reports. Spin-parity assignments of ^{101}Ru levels shown in Figure 18a are based on precision energy and accurate relative intensity data of this investigation, and the previous studies of ^{101}Rh decay (3, 17, 26), Coulomb excitation (49) and ^{100}Mo (α, 3n) reaction (54). It was assumed that gamma-ray transitions observed following the ^{101}Tc decay are limited to M1 and E2 multipolarity.

The Ground State of ^{101}Ru and ^{101}Tc

The ground state of ^{101}Ru has been directly measured by Griffiths and Owen (38) to have spin-parity of $5/2^+$. Its nuclear magnetic dipole moment (μ) was measured by Murakawa (68) to be -0.69 ± 0.15 nm indicated that μ belongs to $d_{5/2}$ Schmidt group. Most nuclei with odd neutrons from 51 to 61 have ground-state spins $5/2^+$. The filling order for 51-61 neutrons as deduced from data of spins, magnetic moments and electric quadrupole moments (62), suggests that the neutron configuration of ^{101}Ru ground state is $(1g_{7/2})^2_{0^+}$ $(2d_{5/2})^5_{5/2^+}$.

In contrast, the ground state of ^{101}Tc has not directly been measured. Previously, spin-parity of the ^{101}Tc ground state has been assigned to a value of $9/2^+$ in analogy to the measured value of ground state spin-parity of ^{99}Tc. According to the extended

quasiparticle-phonon coupling calculations of Goswami and Sherwood (36), the ground state of ^{101}Tc might possibly be $1/2^-$. Shell-model calculation have been performed by Vervier (90) using an exact diagonalization of $(\pi p_{1/2})^1(\pi g_{9/2})^m(\nu d_{5/2})^n$ configuration in order to obtain the level scheme of the Tc isotopes. The ground state configuration of ^{101}Tc is, in analogy to that of ^{99}Tc, $(g_{9/2})^3(d_{5/2})^6$. Therefore, the ground state of ^{101}Tc could be either $(g_{9/2})^3_{9/2^+}$ or $(g_{9/2})^2_{0^+}(p_{1/2})^1_{1/2^-}$. In fact the results of the extended quasiparticle-phonon coupling (EQPC) calculations of Goswami and Sherwood indicate that the $1/2^-$ is lower in energy than the $9/2^+$. The EQPC theory is partially successful in predicting low-lying level of ^{99}Tc, ^{101}Rh and ^{109}Ag, especially the ground and first excited states (35). However, according to the present findings spin-parity of ^{101}Tc ground state cannot possibly be $1/2^-$ but must be $9/2^+$, because beta-transition to $11/2^+$ state of 1001.1 keV and the maximum beta branching (90.3%) to the $7/2^+$ level at 306.8 keV have been observed. Additionally, the new proposed level scheme of ^{101}Tc (Figure 19) confirms the $9/2^+$ spin-parity assignments for the ground state of ^{101}Tc.

The 127.2 keV Level

A $3/2^+$ spin-parity has been well established for this first excited state based on the data from the studies of angular distribution of gamma rays from Coulomb excitation with neon ions (78), from the

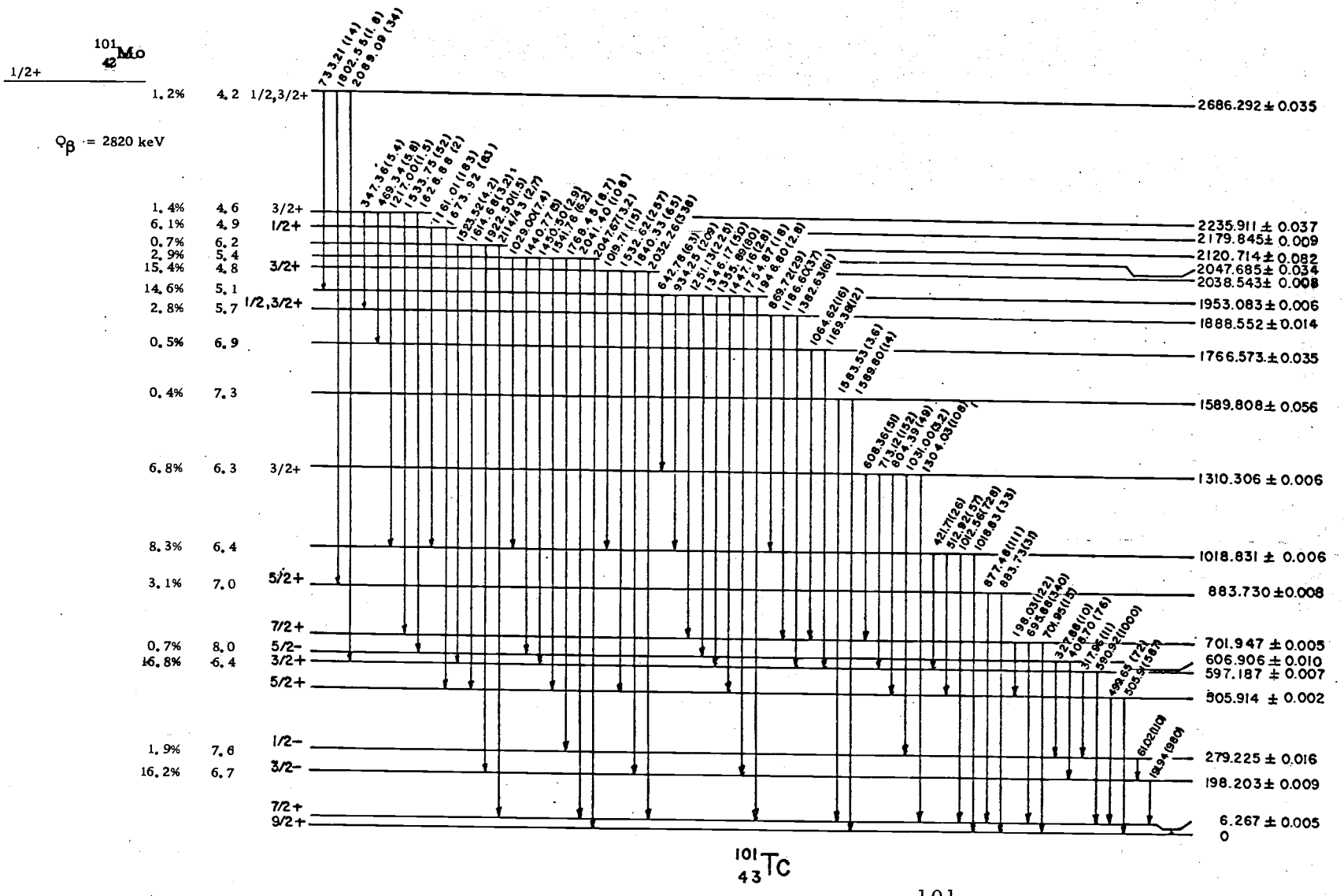

Figure 19. New proposed level scheme of ^{101}Tc.

gamma-gamma directional correlation studies of ^{101}Rh decay(96), and from the M1-E2 multipole order of 127.2 keV transition determined from conversion coefficient measurement (17). The measured lifetime and nuclear magnetic moment of this level are 0.63 ns and -0.11 nm respectively (17).

The 306.8 keV Level

The fact that this level is fed by the allowed beta decay from the $9/2^+$ state of ^{101}Tc as well as the allowed electron capture decay from the $9/2^+$ ^{101m}Rh level and gamma ray transition to the $5/2^+$ ground state is much more intense than that to the $3/2^+$ first excited state, suggest that this level has the spin-parity of $7/2^+$.

The 311.2 keV Level

Since a strong gamma transition between the 311.2 keV and the first excited $3/2^+$ levels has been observed (26), the spin of 311.2 keV level should not be higher than 7/2. Since there is no direct population from ^{101m}Rh or ^{101}Tc, one must have $J \leq 5/2$. Neither 311.2 nor 183.8 keV gamma transitions were observed in the decay of ^{101g}Rh (see Figure 18b), indicated that this level is not populated by the decay of ^{101g}Rh either. This fact rules out the $1/2^+$ and $3/2^+$ choices. Hence, a $5/2^+$ assignment for the 311.2 keV levels is consistent with

all the available data.

The 325.4 keV Level

This level is populated by the decay of ^{101g}Rh ($1/2^-$) only, and for this reason is expected to have a low spin. Electron capture decay from ^{101g}Rh to this state has log ft = 7.5 (3) which indicates a first forbidden transition. Therefore, the spin-parity of 325.4 keV level may be either $1/2^+$ or $3/2^+$. Internal conversion electron data (26) and gamma-gamma directional polarization correlation data (96) on the decay of $1/2^-$ ^{101g}Rh isomer suggested that 198 keV transition is primarily M1. If the 325.4 keV transition exhibited a strong M1 character also it would be expected to dominate the 198 keV transition. The observed relatively low intensity 325.4 keV gamma line (3, 26) strongly supports the assignments of $1/2^+$ for the 325.4 keV level.

The 421.9 keV Level

This level is fed directly by electron capture decay of ^{101g}Rh (3, 17, 26), and, based on this fact, is expected to have spin 3/2 or lower. This expectation is consistent with this study since the level is not directly populated by the beta decay of ^{101}Tc. With additional information on gamma ray branching of the 295 and 421.5 keV transitions deduced from this study and observed by previous workers (3, 17, 26, 49, 50), spin-parity assignments of the 421.9 keV level are

restricted to a value of $3/2^+$.

The 528 keV Level

This isomeric state has been first proposed by Evans and Naumann (26) according to their conversion electron data to be at 523 keV with a spin-parity of $11/2^-$ which is in good agreement with the $11/2^-$ state predicted by the quasiparticle-phonon coupling model of Kisslinger and Sorrensen (47). The lifetime of this state has been measured to be 17 μs (13), 25 μs (63) and 35 μs (43) but the 17 μs is likely an accepted value. Recent nuclear reaction studies of Lederer et al. (54) from the ^{100}Mo (α, 3n) reaction indicated that this $11/2^-$ isomeric state is at 528 keV and is not fed by any gamma transitions from positive parity states. These authors observed that the 528 keV level is populated by an E2 transition from a $15/2^-$ level at 959 keV. Since the beta decay selection rules prohibit beta transitions from $9/2^+$ ^{101}Tc ground state to the $15/2^-$ state, hence the 959 and 528 keV levels are not populated in the decay of ^{101}Tc as one would expect.

The 616.3 and 674.2 keV Levels

Existence of the 616.3 keV level is justified by the presence of a 489.1 keV gamma transition from this state to the $3/2^+$ first excited state and from the fact that the state is fed by the 321.9 keV gamma transition. This confirms a 616.3 keV level observed in Coulomb

excitation studies (49).

Another new level is proposed at 674.2 keV. The principal evidence for the existence of this state is the energy relationship and the intensity balancing. Since both levels are not directly fed by beta decay from ^{101}Tc spin-parity assignments of either $3/2^+$ or $5/2^+$ are suggested for these two levels.

The 720.1, 911.9 and 928.8 keV Levels

These levels are populated directly from ^{101}Tc by allowed beta transitions and decay to lower states having spin 5/2 or larger. Hence spin-parity assignments for these levels are restricted to values of $7/2^+$ or $9/2^+$.

The 842.5 and 938.1 keV Levels

These levels are also fed directly by allowed beta transitions that de-excitation includes transitions to states having spin-parity as low as $3/2^+$. Thus, assignments of spin-parity for these levels are restricted to a value of $7/2^+$.

The 1001.1 keV Level

This is the highest level of ^{101}Ru observed in this study. It has not previously been observed in either ^{101}Tc decay or Coulomb excitation studies. The level is directly excited by beta decay from the

$9/2^+$ ^{101}Tc ground state and de-excites to the 306.8 keV ($7/2^+$) only. This evidence suggests the spin-parity assignments of $11/2^+$ for the level which is in good agreement with a $11/2^+$ level at 1001 keV observed in ^{100}Mo (α, 3n) reaction studies (54).

DISCUSSION AND INTERPRETATION OF LEVELS

A comparison of nuclear level structure of ^{101}Ru proposed on the basis of this study (Figure 18a) compared with those levels found in the previous radioactive decay studies (Figure 4) shows a great deal of improvement. Information pertaining to the low-lying levels of ^{101}Ru from this study is in good agreement with the previous studies of ^{101}Rh decay (3, 17, 26) as is evident from Figure 18. The only levels of ^{101}Ru that are populated by the decay of ^{101}Rh but not by the decay of ^{101}Tc occur at 639 and 325.4 keV.

Fourteen gamma transitions which previously were not observed or were indicated only in coincidence spectra are observed in this study and are well established in the proposed level scheme. These transitions verify a level of ^{101}Ru at 616.3 keV found in Coulomb excitation studies (49) which had not been observed in previous investigations of the decay of ^{101}Tc. In addition, new levels at 674.2, 911.9, 938.1 and 1001.1 keV are proposed. Information as to higher lying levels in ^{101}Ru obtained from this investigation are generally in good agreement with those of Coulomb excitation (49) and nuclear reaction (54) studies. Gamma branching ratios of levels in ^{101}Ru which are populated both in the decay of ^{101}Tc, in the Coulomb excitation or in the ^{100}Mo (α, 3n) reaction are shown in Table 3 for comparison. Weak gamma transitions having energies of 110.7, 114.8, 174.7, and

Table 3. Gamma ray energies and branching ratios from levels observed both in the ^{101}Tc decay, in the Coulomb excitation, or in the (α, 3n) reaction.

Level (keV)	This Study		Kistner and Sorrensen (47)		Lederer et al. (54)	
	E_γ (keV)	γ-branching (%)	E_γ (keV)	γ-branching (%)	E_γ (keV)	γ-branching (%)
127	127.2	100	127.2	100	127.8	100
307	179.3	0.1			179.4	1
	306.8	99.9	306.8	100	307.1	99
311	183.8	93	184.1	87	184.0	100
	311.2	6	311.1	13		
422			110.7	4		
			114.8	2		
	295	64	294.8	62		
	421.9	36	422.0	32		
545	233.6	4	233.7	4		
	238.1	5	238.1	5	238.8	6
	544.8	91	544.9	91	545.8	94
616	489.1	50	489.1	50		
	616.3	50	616.3	50		
720			174.7	8	175.0	17
			408.4	3		
	413.5	4	413.1	6		
	720.1	96	720.1	83	720.6	83
929	384.0	16				
	617.6	16	618	50	618.2	59
	622.0	21				
	928.8	47	928.9	50	929.7	41
1001					70.8	1
					281.2	5
	694.3	100			694.0	94

and 408.4 keV, reported by Kistner and Schwarzschild (49), were not observed in the gamma spectrum of ^{101}Tc. Lederer et al. (54) also indicated weak 70.8 and 281.2 keV transitions, resulting from the de-excitation of the 1001 keV level to the 930 and 720 keV levels. These transitions are too weak to be seen in the gamma spectrum of ^{101}Tc collected in this study. However, later measurements performed with a Compton suppression system confirm the weak gamma lines at 110.8, 115.8, 175.1 and 281.9 keV.

Aras et al. proposed new levels at 639, 953.4, and 1011.5 keV, but the existence of these levels is uncertain. Careful search was made for gamma lines at 332, 408, 953.4 and 1011.5 keV which are the expected transitions from these proposed levels. No evidence of these transitions was found in the uncontaminated ^{101}Tc samples. These transitions, however, have been observed in the gamma-ray spectrum of the ^{101}Mo - ^{101}Tc admixture. It is, therefore, likely that these levels are incorrectly assigned to the level structure of ^{101}Ru.

For the purposes of positive identification of the ^{101}Mo impurity contained in the ^{101}Tc samples and a verification of the $9/2^+$ spin-parity assignments of the ^{101}Tc ground state, precision energy and intensity measurements of gamma rays emitted in the decay of 14.6 minute ^{101}Mo have also been performed. Gamma spectra of ^{101}Mo were recorded shortly after irradiations. The energies and relative

intensities of gamma rays observed in the decay of 14.6 minute ^{101}Mo are listed in Table 4. Prior to the present investigation, the most recent studies of this nuclei were carried out by Cretu et al. (20) utilizing scintillation spectrometers. The decay scheme of ^{101}Mo proposed by these authors is depicted in Figure 20. Based on the results of the present investigation and the selection rules for the beta and gamma decay, a new decay scheme of ^{101}Mo (Figure 19) is proposed. Evidently, the new proposed decay scheme of ^{101}Mo shows a remarkable improvement of the nuclear level structure of ^{101}Tc in comparison with the one previously proposed by Cretu et al. (20)(Figure 20).

Comparison of the energy levels of ^{101}Tc found in this study and those predicted by the theoretical calculations of Goswami and Sherwood (36) and of Begzhanov et al. (7) is shown in Table 5. One sees that levels of ^{101}Tc are poorly understood theoretically.

Aras et al. (2) were able to identify low lying levels of ^{101}Ru based on the model developed by Nilsson (67, 70). In this model, the effect of axially symmetric deformation on shell model states is considered. The pattern of energy levels according to the Nilsson model would take the form of a set of single particle states, with a rotational band superimposed upon each of them. The ground state of ^{101}Ru was assigned to the $5/2^{+}[402]$ Nilsson state, and the excited states were assigned to four rotational bands:

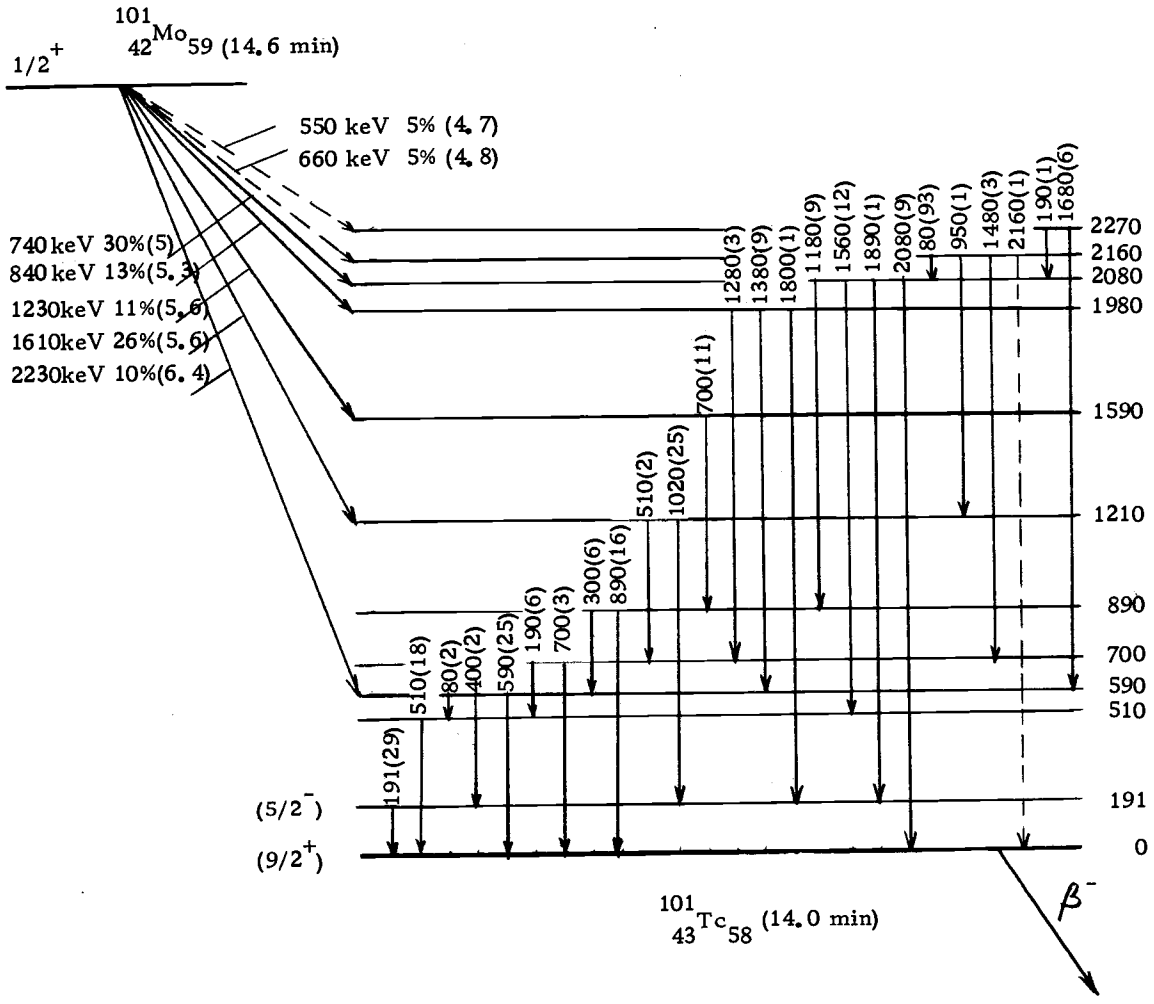

Figure 20. Decay scheme of ^{101}Mo , adopted from Cretu et al. (20).

Table 4. Positions, energies and relative intensities of γ -rays emitted in the decay of 14.6 minute ^{101}Mo.

Transition	Energy (keV)	Relative Intensity
3 → 2	81.02 ± 0.05	110
2 → 1	191.94 ± 0.01	756. ± 15
7 → 4	196.03 ± 0.01	119 ± 6
5 → 3	317.96 ± 0.02	11.0 ± 0.9
6 → 3	327.68 ± 0.03	10.3 ± 0.6
19 → 13	347.36 ± 0.04	5.4 ± 0.5
6 → 2	408.70 ± 0.01	75.5 ± 0.8
9 → 5	421.71 ± 0.03	25.5 ± 0.8
19 → 12	469.34 ± 0.06	5.8 ± 0.9
4 → 1	499.65 ± 0.01	72.0 ± 0.4
4 → 0	505.91 ± 0.01	587 ± 10
9 → 4	512.92 ± 0.01	57.0 ± 1.1
5 → 1	590.92 ± 0.01	1000 ± 25
10 → 7	608.36 ± 0.01	50.5 ± 1.5
14 → 10	642.78 ± 0.01	62.5 ± 2.9
7 → 1	695.68 ± 0.01	340 ± 13
7 → 0	701.95 ± 0.04	14.8 ± 0.8
10 → 5	713.12 ± 0.01	152 ± 7
20 → 14	733.21 ± 0.04	13.9 ± 0.9
10 → 4	804.39 ± 0.02	49.4 ± 4.0
13 → 9	869.72 ± 0.05	29.0 ± 6.6
8 → 1	877.46 ± 0.01	111 ± 22
8 → 0	883.73 ± 0.04	30.8 ± 1.5
14 → 9	934.25 ± 0.01	209 ± 15
9 → 1	1012.56 ± 0.01	728 ± 44
9 → 0	1018.83 ± 0.05	32.7 ± 2.5
15 → 9	1019.71 ± 0.02	15.2 ± 2.3
16 → 9	1029.00 ± 0.17	7.4 ± 2.0
10 → 3	1031.00 ± 0.20	3.2 ± 1.1
12 → 7	1064.62 ± 0.05	16.4 ± 2.4
18 → 9	1161.01 ± 0.01	183 ± 15
12 → 5	1169.38 ± 0.06	12.0 ± 1.7
13 → 7	1186.60 ± 0.02	37.4 ± 1.9
16 → 9	1217.00 ± 0.05	1.5 ± 1.7
14 → 7	1251.13 ± 0.01	225 ± 21
10 → 1	1304.03 ± 0.01	108 ± 22
14 → 6	1346.17 ± 0.02	50.1 ± 3.0
14 → 5	1355.89 ± 0.01	80 ± 9
13 → 4	1382.63 ± 0.02	61 ± 2
16 → 6	1440.77 ± 0.13	5.3 ± 0.9
14 → 4	1447.16 ± 0.20	2.8 ± 0.5
16 → 5	1450.50 ± 0.30	2.9 ± 0.5
17 → 5	1523.52 ± 0.16	4.1 ± 2.8
15 → 4	1532.62 ± 0.01	257 ± 36
19 → 7	1533.75 ± 0.01	53 ± 3
16 → 4	1541.76 ± 0.14	6.2 ± 1.2

Table 4 continued.

Transition	Energy (keV)	Relative Intensity
11 → 1	1583.53 ± 0.17	3.6 ± 0.8
10 → 0	1589.80 ± 0.06	13.6 ± 1.3
17 → 4	1614.68 ± 0.24	3.2 ± 1.0
19 → 6	1628.88 ± 0.29	2.0 ± 0.5
18 → 4	1673.92 ± 0.02	83.0 ± 4.8
14 → 2	1754.87 ± 0.06	18.0 ± 0.6
16 → 3	1768.45 ± 0.11	6.7 ± 1.1
20 → 8	1802.55 ± 0.30	4.9 ± 2.0
15 → 2	1840.33 ± 0.03	65.0 ± 2.5
17 → 2	1922.50 ± 0.32	1.5 ± 0.7
14 → 1	1946.80 ± 0.24	2.8 ± 0.8
15 → 1	2032.26 ± 0.02	338 ± 68
16 → 1	2041.70 ± 0.04	108 ± 3
16 → 0	2047.67 ± 0.25	3.2 ± 0.9
20 → 5	2089.09 ± 0.10	34
17 → 1	2114.43 ± 0.10	27

Table 5. Comparison of level energies of ^{101}Tc: experimental (this study) and theoretical calculations of Goswami and Sherwood and of Begzhanov et al.

This Study		Goswami & Sherwood (36)		Begzhanov et al. (7)	
Level Energy (keV)	J^{π}	Level Energy (keV)	J^{π}	Level Energy (keV)	J^{π}
0	$9/2^+$	0	$1/2^-$	0	9/2
6.267	$7/2^+$	-	-	-	-
-	-	104	$5/2^+, 7/2^+, 11/2^+, 13/2^+$	-	-
198.203	$3/2^-$	-	-	191	5/2
279.225	$1/2^-$	-	-	255	1/2
-	-	-	-	318	3/2
505.914	$5/2^+$	-	-	-	-
597.187	$3/2^+$	590	$3/2^-$	-	-
606.906	$5/2^-$	620	$9/2^+$	-	-
701.947	$7/2^+$	-	-	-	-
883.730	$5/2^+$	800	$5/2^-$	900	7/2
1018.831	-	-	-	-	-
-	-	-	-	1120	3/2
-	-	-	-	1150	5/2
1310.306	$3/2^+$	-	-	-	-
-	-	-	-	1470	9/2
1589.808	-	-	-	-	-
1766.573	-	-	-	-	-
1888.552	$1/2^+, 3/2^+$	-	-	-	-
1953.083	-	-	-	-	-
2038.543	$3/2^+$	-	-	-	-
2047.685	-	-	-	-	-
2120.714	-	-	-	2100	7/2
2179.845	$1/2^+$	-	-	-	-
2235.911	$3/2^+$	-	-	-	-
-	-	-	-	2450	5/2
2686.292	$1/2^+, 3/2^+$				

Energy Level (keV)	Nilsson State $J^{\pi}[Nn_z\Lambda]$
0	$5/2^+[402]$
127.2	$3/2^+[411]$
306.8	$7/2^+[402]$
311.2	$5/2^+[411]$
325.4	$1/2^+[420]$
421.9	$3/2^+[420]$
544.8	$7/2^+[404]$
720.1	$9/2^+[402]$

The above assignments seem to fit the data rather well. However, the findings of Kistner and Schwarzschild (49) indicated, from the deduced values of B(E2), that low-lying levels of ^{101}Ru possess a collective character. This suggests that the assignments of ^{101}Ru levels based on the Nilsson model description are accidentally correct.

The low-lying states in even-even nuclei adjacent to ^{101}Ru have been successfully identified with the collective states in the vibrational model. In this model the nucleus is thought to perform small oscillation about its spherical equilibrium shape. The normal modes of oscillations are labeled by their multipole order λ . Dipole collective oscillations ($\lambda = 1$), which correspond to a displacement of the whole nucleus, cannot occur because of conservation of momentum, and the simplest oscillations have quadrupole character ($\lambda = 2$). The excitation energies of the vibrational levels are evenly spaced, as expected from the excitation of an integral number of "phonons", and are equal to $\sum_{\lambda} N_{\lambda} \hbar\omega_{\lambda}$, where the integer N_{λ} is the number of phonons of order λ in the excited state. A phonon of order λ

carries an angular momentum of λ units and parity $(-1)^{\lambda}$. With the assumption that the oscillator be harmonic, and after taking into account the rules of addition of angular momentum and the restrictions of Bose statistics for the phonons, we obtain the following successive excited states of the nucleus:

State	Number of Phonons	Excitation Energy	Angular Momentum
Ground	0	0	0
First Excited	1	$\hbar\omega$	2
Second Excited	2	$2\hbar\omega$	0, 2, 4
Third Excited	3	$3\hbar\omega$	0, 2, 3, 4, 6

The first excited state has one quadrupole phonon and is a 2^+ state. Collective octupole oscillations ($\lambda = 3$) are also observed. These appear as a low-lying 3^- level in even-even nuclei such as ^{88}Sr or ^{208}Pb. The doubly even core ^{100}Ru has its first excited 2^+ state at 540 keV and its second excited two-phonon states lie at $1132(0^+)$, $1230\ (4^+)$ and $1366\ (2^+)$ keV. The first 2^+ state of ^{102}Ru is at 475 keV whereas its second excited states are almost degenerate at $1103\ (2^+)$ and $1107\ (4^+)$ keV. Low-lying vibrational levels of even-A ruthenium isotopes are shown in Figure 21. It would be interesting to note the lowering trend of the 2^+ state as one goes from ^{96}Ru to ^{104}Ru.

Nuclei of ^{101}Ru are obtained by adding one neutron to the ^{100}Ru (or by subtracting one neutron from the ^{102}Ru) neighboring core. It would be surprising if similar collective features were absent in ^{101}Ru

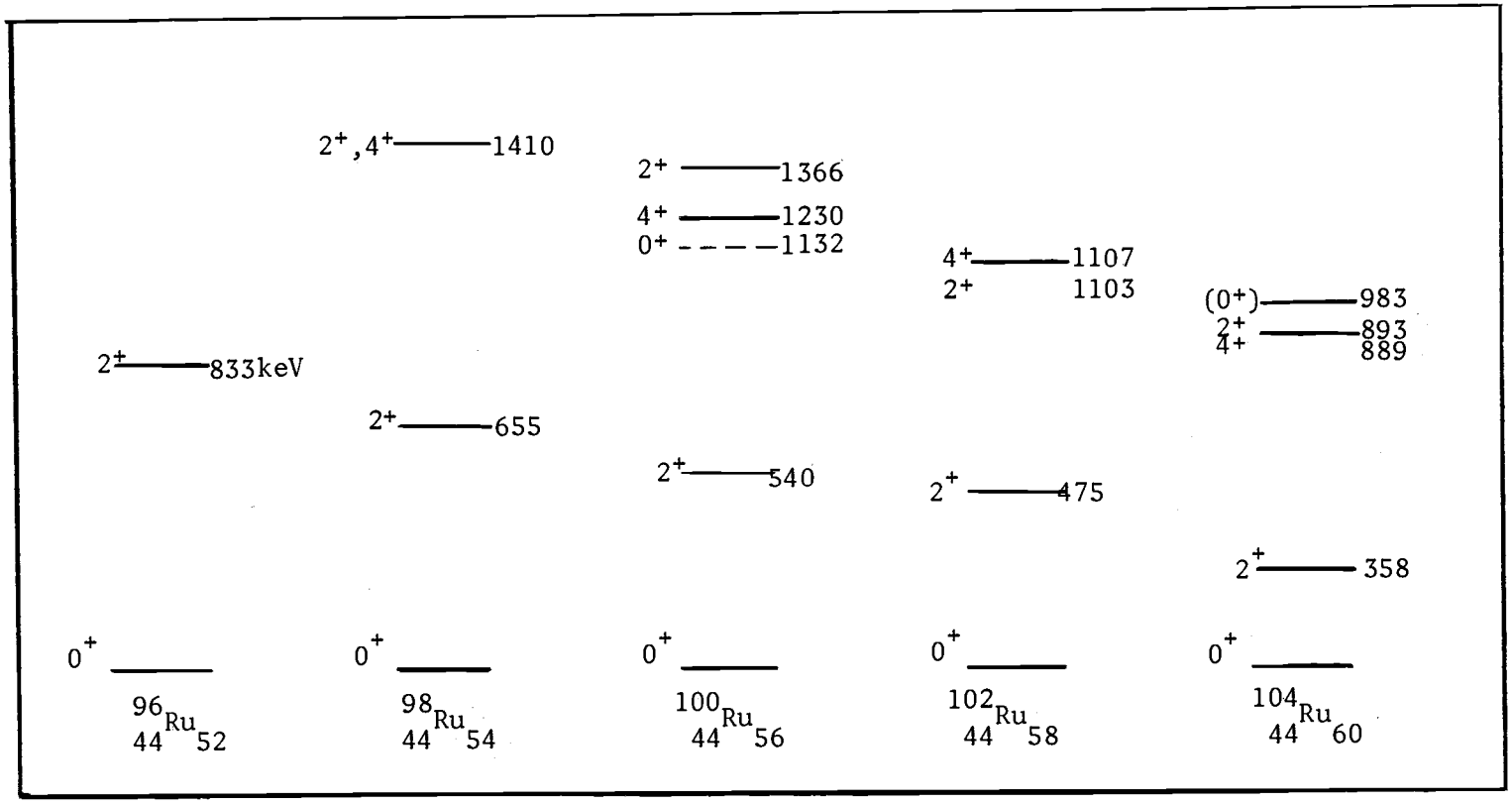

Figure 21. Low-lying levels of even-A ruthenium nuclei, adapted from McGowan et al. (65).

nuclei and other odd-A ruthenium isotopes differing from their doubly even neighboring cores by addition or subtraction of a single neutron. The energy levels of odd-A ruthenium isotopes may be explainable in terms of a weak coupling of the odd neutron with the vibrational phonons of the even-even core. In this respect, the ground state of the odd-A Ru-isotope consists of the odd neutron in its lowest single particle state of the average potential created by the doubly even core. If the next single particle state in this average potential is high compared to the lowest excitation energy of the core, the excited states of the odd-A isotope would result from coupling the odd neutron in its lowest state to the excited states of the core. If J_c is the angular momentum of the core and j is the angular momentum of the odd-neutron outside the core, then for each collective core state there will be a multiplet of states with either $2J_c + 1$ or $2j + 1$ (whichever is smaller) members and spins $J = J_c - j,\ J_c - j + 1,\ \cdots,\ J_c + j$. This model description was proposed by de-Shalit (21) in 1961. The interaction between the odd particle and the core is taken to be the scalar product of two tensors of rank k: $T^{(k)}(c)$ operating on the core degree of freedom and $T^{(k)}(p)$ operating on the degree of freedom of the particle. Since the particle-core interaction does not involve the monopole ($k = 0$) terms, the center of gravity theorem of Lawson and Uretsky (51) states that the center of gravity of each multiplet of states arising from a particular J_c lies at roughly the same energy

as the state J_c of the doubly even core.

It is instructive to distinguish the positive from the negative parity states when discussing the nature of the states of ^{101}Ru nuclei. Four negative parity states of ^{101}Ru have been observed in the ^{100}Mo(α, 3n)^{101}Ru reaction studies of Lederer et al. (54). These authors observed a strong cascade feeding the well-known $11/2^-$ isomeric state:

$$2445(23/2^-) \xrightarrow{E2} 1594(19/2^-) \xrightarrow{E2} 959(15/2^-) \xrightarrow{E2} 528(11/2^-),$$

and the energies and angular distributions of these transitions bear a strong resemblance to those of the dominant $6^+ \rightarrow 4^+ \rightarrow 2^+ \rightarrow 0^+$ cascade observed in their studies of the ^{98}Mo(α, 2n)^{100}Ru reaction. They postulate that the 959-, 1594- and 2445 keV states of ^{101}Ru could be the maximum spin members of the multiplets formed from one-, two-, and three phonon excitations coupled to the $h_{11/2}$ neutron state. Although the single particle $h_{11/2}$ neutron state lies at very high energy (~ 2.7 MeV) and lower spin members of the multiplets have not been observed, the weak coupling model of de-Shalit may have some validity in the negative parity states of ^{101}Ru.

The positive parity states are considered next and the presently available experimental information on the positive parity levels of $^{97\text{-}103}$Ru is summarized in Figure 22. These odd-A ruthenium

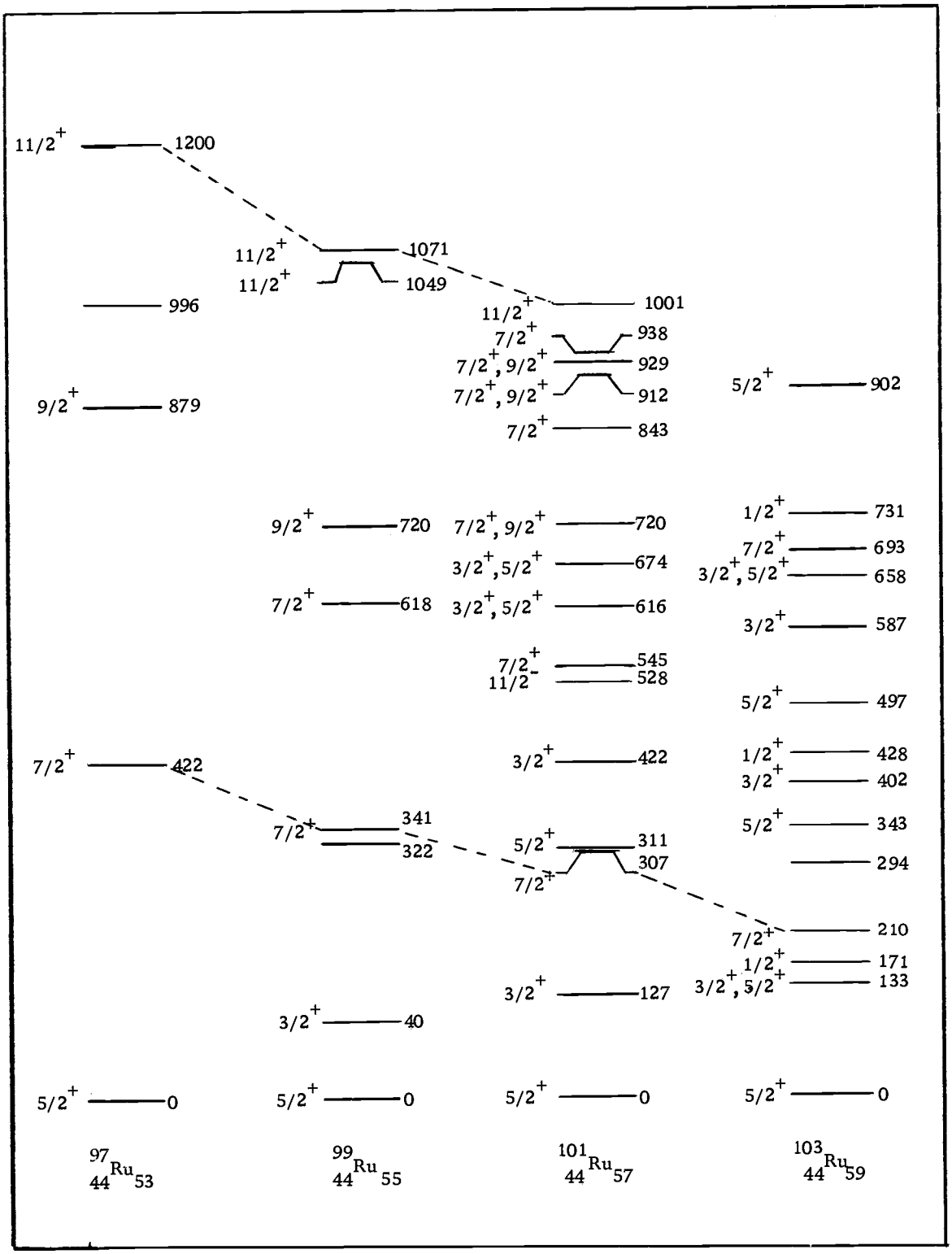

Figure 22. Comparison of positive parity levels of $^{97\text{-}103}$Ru (below 1200 keV). The data are compiled from this study and references 22 and 54.

isotopes all have ground spin state $5/2^+$ if core excitation picture of de-Shalit is applicable to these nuclei; one would then expect to observe a quintet with $1/2^+ \leq J^\pi \leq 9/2^+$ resulting from the coupling of $d_{5/2}$ single-particle neutron state to the 2^+ one phonon state of the doubly even core. The center of gravity of the multiplet should lie near the 2^+ state of the neighboring doubly even nuclei.

If the 720.1 ($9/2^+$), 544.8 ($7/2^+$), 421.9 ($3/2^+$), 311.2 ($5/2^+$) and 325.4 ($1/2^+$) keV states of ^{101}Ru are chosen to be the members of the quintet, the calculated center of gravity of the multiplet is 526 keV. However, if the 127.2 keV is substituted for the 421.9 keV as the $3/2^+$ member, one would obtain the calculated center of gravity at 486 keV. Likewise, the center of gravity of the multiplet will be 462 keV if the 306.8 keV is chosen for the $7/2^+$ member. Hence, the center of gravity of the multiplet lies between the first 2^+ state of ^{100}Ru and the first 2^+ state of ^{102}Ru depending on what choices are made for the $7/2^+$ and $3/2^+$ members. The occurrence of two levels having the same j poses a severe problem for the core excitation picture, since only one level of each spin is predicted. As pointed out by Aras et al. (3) that the 127.2 and 306.8 keV have pronounced single particle character, hence, these two states should be excluded from the core multiplet.

Black et al. (10) have interpreted the higher multiplet in ^{103}Rh as arising from coupling of the $p_{1/2}$ state to the two-phonon core

states. A similar situation may occur in ^{101}Ru, levels at 1001.1 ($11/2^+$) 938.1 ($7/2^+$) and 928.8 ($9/2^+$) keV may be thought of as three members of the multiplet formed through the coupling of the $d_{5/2}$ neutron to the 4^+ state of the ^{100}Ru core ($4^+ + d_{5/2} \rightarrow 13/2^+$, $11/2^+$, $9/2^+$, $7/2^+$, $5/2^+$, $3/2^+$). The 674.2 and 616.3 keV states could possibly be the $3/2^+$ and $5/2^+$ members of this multiplet. The 842.5 keV level has not been observed in Coulomb excitation studies and should have no collective characteristics. This level could possibly be a single-particle state of the $(d_{5/2})^6_{0^+}$ $(g_{7/2})^1_{7/2^+}$ neutron configuration. However, according to the positions of single-particle levels in this region of odd-A nuclei as shown in Table 1 of reference 36, the low-lying level of ^{101}Ru cannot be described by the simple shell model. The neutron single particle energies for the $d_{5/2}$ and $g_{7/2}$ are at 559 and 947 keV. The $s_{1/2}$, $h_{11/2}$ and $d_{3/2}$ single particle states which lie within the same major shell (N = 50-82) are at 2034, 2724 and 3438 keV respectively which are more than 1500 keV above the $d_{5/2}$ state. There are, however, 15 levels in ^{101}Ru below 1002 keV, hence, there must be, as is evident from the above discussion, some collective excitation associated with these levels, and core excitation description must have some validity in the levels of ^{101}Ru.

Core excitation concept is included in the quasiparticle-phonon coupling (QPC) model of Kisslinger and Sorrenson (47). In the QPC

calculations of Kisslinger and Sorrensen (hereafter referred to as KS), the Hamiltonian of the system is composed of three parts:

$$H = U + \sum_{\alpha} E_a a^{\dagger}_{\alpha} a_{\alpha} + H_{int} ,$$

where U is the constant ground state energy, E_a is the quasiparticle energy, $a^{\dagger}_{\alpha}, a_{\alpha}$ are the quasiparticle creation and annihilation operators[4] and H_{int} is the residual quasiparticle interaction which is taken to be the pairing plus quadrupole force. For the odd-mass nuclei, one has to diagonalize the quasiparticle Hamiltonian in a suitable chosen basis. In the KS calculations only an approximately orthornormal basis was used and they limited their considerations to one quasiparticle and zero-, one- and two phonon excitations only. The effect of the approximately orthonormal basis used in their calculations is that only a part of the quasiparticle interaction can be accounted for. The KS prediction of energy level diagram of ^{101}Ru is in rather poor agreement with the experimental data although the $11/2^-$ isomeric state is correctly predicted. A serious failure of the KS calculations is its inability to predict the $5/2^+$ ground state and the low-lying $7/2^+$ state in ^{101}Ru. Later QPC calculations of Kisslinger (48) where three quasiparticle states are included revealed

---

[4] Mathematical aspects of these operators are quantitatively described in references 14 and 69.

that when a high-spin level lies closed in energy to several low-spin levels of the opposite parity, then, when the level is about half full, the (j-1) member of a three-quasiparticle configuration may occur at very low energy. This seems to be the case in the 50-82 neutron shell since the $9/2^-$ level exists at about 200 keV above the $11/2^-$ isomer in ^{125,127}Te(53). However, this does not seem to be the case for ^{101}Ru nuclei, since there are only seven neutrons beyond the closed shell of 50 and the $h_{11/2}$ neutron shell lies more than 1500 keV above the $d_{5/2}$ shell.

In the KS calculations only part of the quasiparticle Hamiltonian is assumed to be important and as a consequence it neglects important parts of the quasiparticle interaction. These neglected parts are included in the calculations of Sherwood and Goswami (81) by extending the orthonormal basis to include the backward going amplitude terms[5] so that the entire quasiparticle Hamiltonian can be diagonalized (i.e., all of the quasiparticle interaction are accounted for). The QPC calculations in which the extended basis is used are called the extended quasiparticle phonon coupling theory (EQPC). Sherwood and Goswami have shown that as a result of this backward coupling amplitudes the $9/2^+$ quasiparticle level is pushed up in the vicinity of the phonon levels, thus accounting for the appearance of low-lying

---

[5] See references 36 and 81 for more information regarding the mathematical descriptions of these terms.

$7/2^+$ and $5/2^+$ state in the Tc isotopes. In their subsequent paper (36), it has been shown that the $9/2^+ - 1/2^-$ separation in Tc isotopes could also be accounted for. Comparison of the experimental nuclear level structure of ^{101}Ru with the results of the QPC theory of KS and with the results of the EQPC theory of GS (36) is shown in Figure 23.

In Figure 23, it is evident that due to the anomalous features of the level structure of ^{101}Ru: (i) high density of low-lying levels, (ii) close occurrence of levels having the same j, the level structure of ^{101}Ru cannot be fitted by the QPC model of KS. It seems that these anomalous features could be reproduced in the EQPC model since almost all levels of ^{101}Ru below 700 keV have been accounted for in the EQPC calculations of GS although the level positions are somewhat incorrectly reproduced. The wrongly given lowest $7/2^+$ state is probably responsible for the disagreement in the other level positions. In order to get the correct level spacing of $5/2^+ - 7/2^+$ Goswami and Sherwood suggest that a more realistic quasiparticle interaction such as the spin-flip quadrupole forces formerly suggested by Kisslinger (46), as well as a larger number of phonon levels should be used.

In spite of its success in analysis of the Tc isotopes (except possibly ^{101}Tc), the EQPC methods of Goswami and Sherwood faces a serious difficulty in explaining the low-lying levels of Ru, Rh and Ag isotopes. This stems from the fact that whereas $7/2^+$ and $5/2^+$ levels

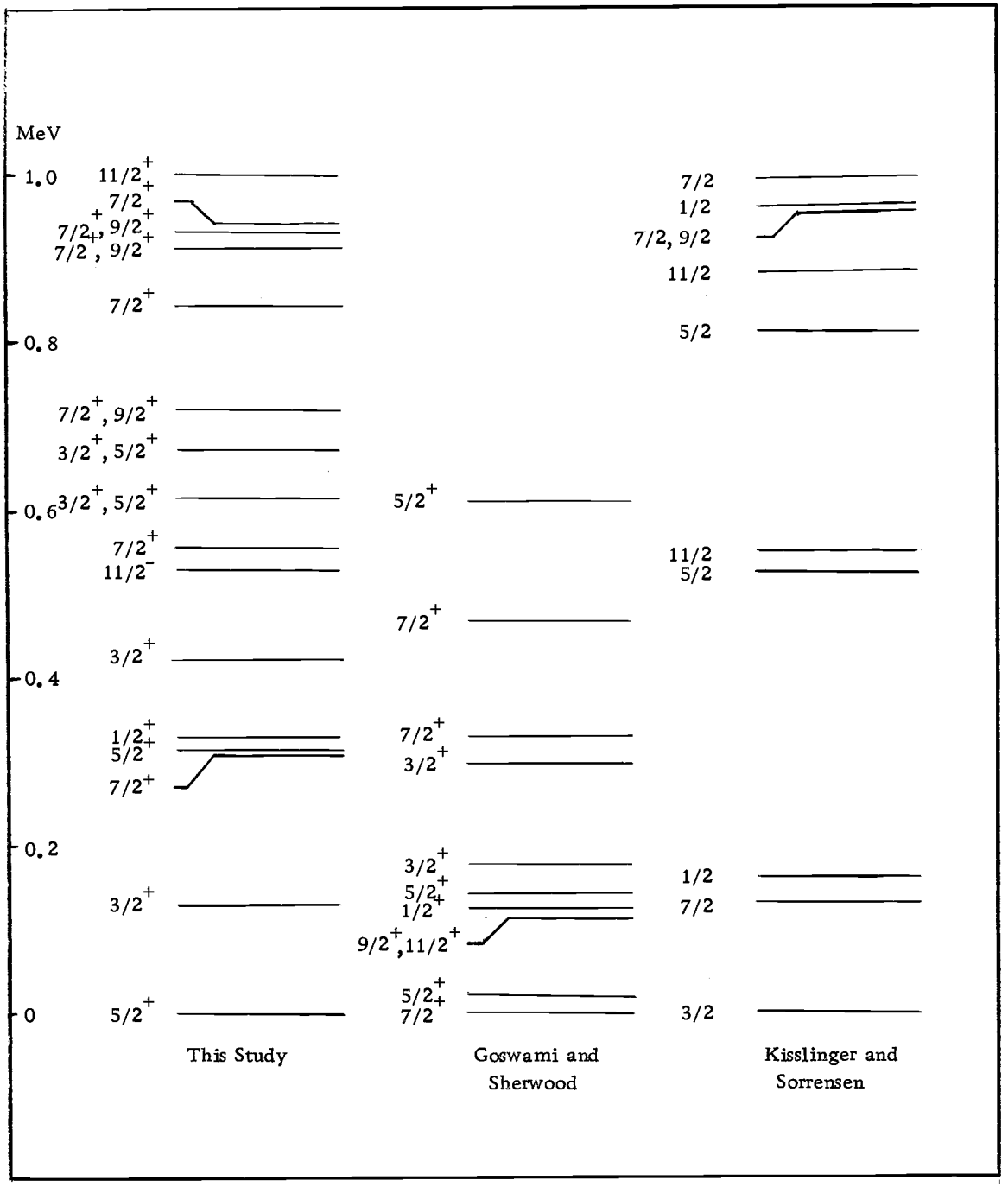

Figure 23. Comparison of ^{101}Ru energy levels: the experimental results of this study and the theoretical predictions of Goswami and Sherwood (36), and Kisslinger and Sorrensen (47).

are nearly degenerate in ^{99}Tc as is expected in the EQPC theory, these two levels are split by ~ 300 keV in ^{99}Ru, ^{101}Ru and ^{101}Rh. In the Ag isotopes the splitting is ~ 600 keV which is somewhat larger than can be expected from the mixing of two and three phonon levels. This splitting of $7/2^+$ and $5/2^+$ levels with increasing Z is a systematic feature and increases gradually as one goes from Tc to the Ag-isotopes. Phelps and Sarantites (75) have pointed out a similarity in trend of this splitting in the Rh isotopes with increasing N. However, in the Ru isotopes the splitting of $7/2^+$ - $5/2^+$ levels decreases with increased N as one goes from ^{97}Ru to ^{103}Ru in a similar manner to the decreasing separation of the first 2^+ states of the doubly even $^{96\text{-}104}$Ru isotopes.

The discovery of large, negative quadrupole moments [~ $\sqrt{B(E2)}$] for the 2^+ phonons of ^{114}Cd and ^{116}Cd (82, 83, 85, 86) has led Goswami and Nalcioğlu (35) to include the effect of the coupling to the quadrupole moment of the core in their EQPC calculations. The experimental values of quadrupole moment of the core is used for evaluating the core matrix element instead of the conventional random phase approximation (RPA) method. Goswami and Nalcioglu were thus able to account for the behaviour of the $5/2^+$ and $7/2^+$ and low-lying levels in the ^{101}Rh and ^{109}Ag nuclei. However, the EQPC theory of Goswami and Nalcioğlu (35) has also predicted the $13/2^+$ and $11/2^+$ to lie very low in the ^{99}Tc, ^{101}Rh and ^{109}Ag isotopes but such states have

not been observed. In their calculations on the ^{99}Tc and ^{101}Rh nuclei the experimental value of -0.6 barns was used for the quadrupole moment of the 2^+ state in ^{104}Ru which is probably larger than the quadrupole moment of ^{98}Ru and ^{100}Ru. This can be inferred from the Coulomb excitation work of McGowan et al. (65) who observed increased $B(E2, O^+ \rightarrow 2^+)$ values by a factor of 3.0 in going from ^{96}Ru to ^{104}Ru. If these authors had used the smaller values for the quadrupole moment of ^{98}Ru and ^{100}Ru doubly even cores in their calculation for ^{99}Tc and ^{101}Rh the agreement with the experimental data may be worse. Recently, McDonald et al. (64) reported the evidence of oblate deformation in the nuclei of ^{99}Tc and indicated that the Nilsson model has some success in predicting the level structure of ^{99}Tc. It would be of best interest to the alert nuclear theoreticians to investigate the validity of the EQPC theory of Goswami and Nalcioğlu in the odd mass ruthenium isotopes particularly the ^{99}Ru and ^{101}Ru nuclei which possess a very complex nuclear level structure.

Failure of the EQPC calculations of Goswami and Sherwood in explaining the first excited and ground states of both the ^{101}Tc and ^{101}Ru nuclei could possibly mean that these nuclei may be slightly deformed from spherical shape similar to the ^{99}Tc nuclei. Regardless of the results of their calculations, Goswami and Sherwood (36) concluded that the most probable spin assignment of the first two states of ^{101}Tc is ground spin $7/2^+$ with first excited state $1/2^-$ so

that the millisecond lifetime of the excited state is explainable from the E3 nature of the transition. However, recent studies on the 191 keV isomeric state of ^{101}Tc by Gabsdil (34) indicate that the nature of the 191 keV transition is predominantly M2. In the calculations of Begzhanov et al. (7), nuclei of ^{101}Tc were considered as being slightly deformed and their prediction of the first two states of ^{101}Tc is in good agreement with the experimental data.

In conclusion, it is evident that certain sets of levels in ^{101}Ru exhibit collective characteristics as is apparent from their selective mode of decay, enhanced B(E2) values, ease of excitation by charged particle bombardment, and the pattern of the cascade. Its exact collective nature, however, is poorly understood. The EQPC theory seems to have certain validity in the odd mass isotopes in this region but more sophisticated theory is required for the ^{101}Ru nuclei. What is clear is that none of the presently existing nuclear models is capable of explaining successfully the complete nuclear level structure of ^{101}Ru and a great deal of further experimental as well as theoretical work on this fascinating nuclei is required.

BIBLIOGRAPHY

1. Antman, S. O. W., D. A. Landis and R. H. Pehl. Measurements of the Fano factor and the energy per hole-electron pair in germanium. Nuclear Instruments and Methods 40:272-276. 1966.

2. Aras, N. K., G. D. O'Kelley and G. G. Chilosi. Energy levels in ^{101}Ru. 1965. p. 13-15. (Oak Ridge National Laboratory Report ORNL-3832.) (microfiche)

3. Aras, N. K., G. D. O'Kelley and G. G. Chilosi. Nuclear levels of ^{101}Ru populated in the decay of ^{101}Rh isomers. Physical Review 146:869-876. 1966.

4. Aubin, G. et al. Calculated relative efficiency for coaxial and planar Ge(Li) detectors. Nuclear Instruments and Methods 76: 85-92. 1969.

5. Aubin, G. et al. Precision measurement of gamma-ray intensities in the decay of $^{152g,\ 154}$Eu, ^{56}Co, ^{110m}Ag and ^{125}Sb. Nuclear Instruments and Methods 75:92-99. 1969.

6. Barnes, Walter Earl. The decay of Pd^{109}, Pd^{111g}, and Pd^{111m}. Doctoral dissertation. Corvallis, Oregon State University, 1971. 133 numb. leaves.

7. Begzhanov, R. B. et al. Excited states of slightly deformed odd nuclei. Akademii Nauk Uzbekskoi Izveztiia SSR 1:60-69. 1967.

8. Birks, J. B. The theory and practice of scintillation counting. New York, Macmillan, 1964. 662 p.

9. Blachot, J., J. A. Pinston and F. Schussler. Desintegration des isomeres du ^{102}Tc. Nuclear Physics A139:434-450. 1969.

10. Black, J. L., W. J. Caelli and R. B. Watson. The low-lying excited states of ^{103}Rh. Nuclear Physics A125:545-567. 1969.

11. Blankenship, J. S. and C. H. Nowlin. New concepts in nuclear pulse amplifier design. IEEE Transactions on Nuclear Science NS-13(3):495-501. 1966.

12. Brahmavar, S. M., J. H. Hamilton and A. V. Ramayya. The decay of ^{110m}Ag: Gamma-ray energy and intensity standardization. Nuclear Physics A125:217-226. 1969.

13. Brandi, K., et al. Investigation of short-lived isomeric states with half-lives in the ns and ms region. Nuclear Physics 59:33-35. 1964.

14. Brown, G. E. Unified theory of nuclear models and forces. New York, John Wiley, 1967. 259 p.

15. Camp, David D. Applications and optimization of the lithium drifted germanium detector system. 1967. 100 p. (University of California Lawrence Radiation Laboratory, Livermore, California. Report UCRL-50156.)

16. Chapman, G. T. Gamma-ray attenuation coefficient for germanium. Nuclear Instruments and Methods 52:101-103. 1967.

17. Connors, Phillip Irving. Properties of the low-lying states in Ru^{99} and Ru^{101}, including the lifetime and magnetic moment of the 127 keV state in Ru^{101}. Doctoral dissertation, University Park, The Pennsylvania State University, 1966. 68 numb. leaves. (microfilm)

18. Cook, W. B., L. Schellenberg and M. W. Johns. The decay of 67 hour ^{99}Mo. Nuclear Physics A139:277-288. 1969.

19. Cretu, T. and L. Funke. Uber den zerfall von Tc^{101} (14 min). Revue Roumaine (de) Physique 10:67-76. 1965.

20. Cretu, T., K. Hohmuth und J. Schintmeister. Gamma messunger zum zerfall von Mo^{101}. Revue Roumaine (de) Physique 11:143-151. 1966.

21. de-Shalit, A. Core excitations in nondeformed, odd-A nuclei. Physical Reviews 122:1530-1536. 1961.

22. Diehl, R. C., et al. Nuclear structure studies with (d, t) reactions on ^{110}Pd, ^{108}Pd, and ^{104}Ru. Physical Reviews C1:2086-2095. 1970.

23. Donnelly, D. P. et al. The calibration of a Ge(Li) gamma-ray spectrometer for energy and relative intensity measurements. Nuclear Instruments and Methods 57:219-226. 1967.

24. DuMond, J. W. M. A high resolving power, curved-crystal focusing spectrometer for shortwave-length x-rays. Review of Scientific Instruments 18:626-638. 1947.

25. Dzhelepov, B. S. et al. Investigation of the decay of Pd^{101}, Rh^{101*}, and Rh^{101}. Soviet Physics - Doklady 10:20-23. 1965. (Translated from Doklady Akademii Nauk SSSR, Vol. 160, no. 1, January, 1965, p. 57-60.)

26. Evans, J. S. and R. A. Naumann. Decay of Rh^{101m} and Rh^{101g}. Physical Review 140:B559-B562. 1965.

27. Ewan, G. T. and A. J. Tavendale. High-resolution studies of gamma-ray spectra using lithium-drift germanium gamma-ray spectrometers. Canadian Journal of Physics 42:2286-2331. 1964.

28. Fairstein, E. and J. Hahn. Nuclear pulse amplifiers, fundamentals and design practice (part 3). Nucleonics 23:50-55. 1965.

29. Fano, U. Ionization yield of radiations. II. The fluctuations of the number of ions. Physical Review 72:26-29. 1947.

30. Faria, N. V. De Castro, and R. J. A. Levesque. Photopeak and double-escape peak efficiencies of germanium lithium drift detectors. Nuclear Instruments and Methods 46:325-332. 1967.

31. Farmer, D. J. Decay of neutron deficient rhodium isotopes. Physical Review 99:679(V7). 1955.

32. Freck, D. V. and J. Wakefield. Gamma-ray spectrum obtained with a lithium-drifted p-i-n junction in germanium. Nature 193:669. 1962.

33. Freeman, J. M. and J. G. Jenkin. The accurate measurement of the relative efficiency of Ge(Li) gamma-ray detectors in the energy range 500 to 1500 keV. Nuclear Instruments and Methods 43:269-277. 1966.

34. Gabsdil, W. The Isomers ^{101m}Tc, ^{158}Tb and ^{208m}Bi. Nuclear Physics A120:555-560. 1968.

35. Goswami, A. and O. Nalcioğlu. Quadrupole moment of the 2^+ phonon and the structure of the odd mass spherical nuclei. Physics Letters 26B:353-356. 1968.

36. Goswami, A. and A. I. Sherwood. Low energy spectra of odd-mass Tc and Ru isotopes. Physical Review 161:1232-1235. 1967.

37. Goulding, F. S. Semiconductor detectors for nuclear spectrometry, I. Nuclear Instruments and Methods 43:1-54. 1966.

38. Griffiths, J. H. E. and J. Owen. The nuclear spins of ^{99}Ru and ^{101}Ru. Proceedings of Physical Society (London) 56A:951-952. 1952.

39. Hahn, J. and R. Mayer. A low noise high gain band width charge sensitive preamplifier. IRE Transactions on Nuclear Science, NS-9(4):20-28. 1962.

40. Heath, R. L., W. W. Black and J. E. Cline. Designing semiconductor systems for optimum performance. Nucleonics 24(5):52-56. 1966.

41. Hollander, J. M. The impact of semiconductor detectors on gamma-ray and electron spectroscopy. Nuclear Instruments and Methods 43:65-190. 1966.

42. Hotz, H. P., J. M. Mathiesen and J. P. Hurley. Calculated efficiencies of Ge(Li) detectors. Nuclear Instruments and Methods 43:65-109. 1966.

43. Ivanov, E. A. Nuclear isomers with half-lifes in the 30-3000 ns range excited in 24 MeV alpha-particle bombardment on natural targets. Revue Roumaine (de) Physique 12:820-838. 1967.

44. Johnson, Ralph A. Resolving radionuclide binary mixtures with a linear equation involving decay measurements in two spectral channels: applications to the ^{101}Mo-^{101}Tc system. Radiochemica Acta 5:231-233. 1966.

45. Kane, W. R. and M. A. Mariscotti. An empirical method for determining the relative efficiency of a Ge(Li) gamma-ray detector. Nuclear Instruments and Methods 56:189-196. 1967.

46. Kisslinger, L. S. The effect of spin-dependent forces on collective motion in nuclei. Nuclear Physics 35:114-135. 1962.

47. Kisslinger, L. S. and R. A. Sorrenson. Spherical nuclei with simple residual forces. Reviews of Modern Physics 35:853-915. 1963.

48. Kisslinger, L. S. A note on coupling schemes in odd-mass nuclei. Nuclear Physics 78:341-352. 1966.

49. Kistner, O. C. and A. Schwarzschild. Coulomb excitation of ^{99}Ru and ^{101}Ru. Physical Reviews 154:1182-1192. 1967.

50. Konijn, J. et al. The decay of the isomers of ^{102}Rh. Nuclear Physics A138:514-528. 1969.

51. Lawson, R. D. and J. L. Uretsky. Center of gravity theorem in nuclear spectroscopy. Physical Reviews 108:1300-1304. 1957.

52. Lingeman, E. W. A. et al. The decay of ^{214}Pb and other ^{226}Ra daughters. Nuclear Physics A133:630-647. 1969.

53. Lederer, C. M., J. M. Hollander and I. Perlman. Table of isotopes. Sixth edition. New York, Wiley, 1967. 594 p.

54. Lederer, C. M., J. M. Jacklevic and J. M. Hollander. Levels of $^{97, 99, 101}$Ru populated in (α, xn) reactions. 1969. (Nuclear Chemistry Annual Report UCRL-19530.)

55. Malm, H. L. and I. L. Fowler. Large volume coaxial germanium gamma-ray spectrometers. IEEE Transactions on Nuclear Science, NS13:62-71. 1966.

56. Malm, H. L., A. J. Tavendale and I. L. Fowler. A large-volume, coaxial lithium-drift, germanium gamma-ray spectrometer. Canadian Journal of Physics 43:1173-1181. 1965.

57. Mann, H. M. Germanium gamma-ray spectrometers. IEEE Transactions on Nuclear Science NS-14(6):10-26. 1967.

58. Mann, H. M., H. R. Bilger and I. S. Sherman. Observations on the energy resolution of germanium detectors for 0.1-10 MeV gamma rays. IEEE Transaction on Nuclear Science NS-13(3):252-255. 1966.

59. Martin, D. W., S. B. Burson and J. M. Cork. Decay of Mo^{101} (14.6 min). Bulletin of the American Physical Society 1:329. 1956.

60. Mattauch, J. H. E., W. Thiele and A. H. Wapstra. Adjustment to relative atomic masses. Nuclear Physics 67:73-120. 1965.

61. Mayers, J. W. Semiconductors for nuclear spectrometry, II. Nuclear Instruments and Methods 43:55-64. 1966.

62. Mayer, M. G. and J. H. D. Jensen. Shell closure and jj coupling. In: alpha-, beta- and gamma-ray spectroscopy, ed. by K. Siegbahn, Vol. I. Amsterdam, North Holland, 1965. p. 557-582.

63. McCarthy, A. L., B. L. Cohen, and L. H. Goldman. Isomers with half-lives in the range 5-1000 microseconds observed in pulsed 15-MeV deuteron beam bombardment of natural elements. Physical Review 137:B250-B265. 1965.

64. McDonald, J., A. Backlin and S. G. Malmskog. Transition probabilities in ^{99}Tc. Nuclear Physics A162:365-375. 1971.

65. McGowan, F. K. et al. Coulomb excitation of states in the even mass ruthemium nuclei with ^{16}O and ^{4}He ions. Nuclear Physics A113:529-542. 1968.

66. Moszkowski, S. A. A rapid method of calculating log(ft) values for beta transitions. Physical Review 82:35-37. 1951.

67. Mottelson, B. R. and S. G. Nilsson. The intrinsic states of odd -A nuclei having ellipsoidal equilibrium shape. Danske Videnskabernes Selskab, Copenhagen. Matematish-fysiske skrifter. Vol. 1, no. 8, 1959. 105 p.

68. Murakawa, K. Hyperfine structure of the spectrum of ruthenium (part III). Journal of Physical Society of Japan 10:919-926. 1955.

69. Nathan, O. and S. G. Nilsson. Collective nuclear motion and the unified model. In: alpha- beta and gamma-ray spectroscopy, ed. by K. Siegbahn, Vol. I. Amsterdam, North Holland, 1965. p. 601-700.

70. Nilsson, S. G. Binding states of individual nucleon in strongly deformed nuclei. Danske Videnskabernes Selskab, Copenhagen. Matematish-fysiske meddelelser. Vol. 29, no. 16, 1965. 48 p.

71. O'Kelley, G. D., Q. V. Larson, and G. E. Boyd. Decay chain Mo^{101}-Tc^{101}. American Physical Society Bulletin 1:24(G5). 1957.

72. Paradellis, T., and H. Hontzeas. Gamma decay of ^{75}Se. Nuclear Physics A131:378-384. 1969.

73. Paradellis, T. and S. Hontzeas. A semi-empirical efficiency equation for Ge(Li) detectors. Nuclear Instruments and Methods 73:210-214. 1969.

74. Pehl, R. H. and F. S. Goulding. Recent observations on the Fano factor in Ge. Nuclear Instrumentation and Methods 81:329. 1970.

75. Phelps, M. E. and D. G. Sarantites. Level structure of ^{101}Rh from the decay of 8.5h ^{101}Pd. Nuclear Physics A159:113-142. 1970.

76. Radeka, Veljko. Low-noise preamplifiers for nuclear detectors. Nucleonics 23:52-55. 1965.

77. Raeside, D. E. Precision gamma-ray energies in the energy interval between 45 and 1275 keV. Nuclear Instruments and Methods 87:7-11.

78. Ritter, R. C. et al. Coulomb excitation with Ne^{20} ions. Physical Review 128:2320-2331. 1962.

79. Rutledge, W. C., J. M. Cork, and S. B. Burson. Gamma-rays associated with selected neutron-induced radioactivities. Physical Review 85:775-786. 1952.

80. Sanborg, A. O. and J. W. Orth. Relative full energy efficiencies of Ge(Li) detectors of various shape and volumes. Society for Applied Spectroscopy. 7th National Meeting, May 13-17, 22 (no. 4): p. 370. 1968.

81. Sherwood, Arnold I. and Amit Goswami. Extended quasiparticle phonon coupling theory for odd-mass spherical nuclei. Nuclear Physics 89:465-480. 1966.

82. Shilling, G. et al. Static quadrupole moment of the 2^+ state in ^{114}Cd. Physical Review Letters 19:318-321. 1967.

83. Simpson, J. J. et al. A determination of quadrupole moments in ^{114}Cd, ^{130}Ba, ^{148}Sm and ^{150}Sm. Nuclear Physics A94:177-191. 1967.

84. Slater, David N. Gamma rays of radionuclides in order of increasing energy. London, Butterworths, 1962. 201 p.

85. Stelson, Paul H. Coulomb excitation with heavy ions. 1965, p. 1005-1044. (Brookhaven National Laboratory Report BNL948.) (microfiche)

86. Stokstad, R. G. et al. The determination of the static quadrupole moments of the first 2^+ states in ^{114}Cd and ^{116}Cd by higher order effects in Coulomb excitation. Nuclear Physics A92:319-344. 1967.

87. Tavendale, A. J. Large germanium lithium drift p-i-n diodes for gamma-ray spectroscopy. IEEE Transactions on Nuclear Science NS-12(1):255-259. 1965.

88. Temmer, G. M. and N. P. Heydenburg. Coulomb excitation of medium weight nuclei. Physical Review 104:967-980. 1956.

89. Tokcan, G. and C. R. Cothern. Precise form of the efficiency equation for a Ge(Li) detector. Nuclear Instruments and Methods 64:219-220. 1968.

90. Vervier, J. Effective nucleon-nucleon interactions in the Y, Zr, Nb, Mo and Tc isotopes. Nuclear Physics 75:17-18. 1966.

91. Wiles, Donald R. Search for the $p_{1/2}$ isomeric state in ^{101}Tc and identification of energy levels. Physical Review 93:181-182. 1954.

92. Walker, Donald Arthur. The decay of ^{61}Cu and ^{69}Cu--energy levels of ^{61}Ni and ^{59}Ni. Doctoral dissertation. Corvallis, Oregon State University, 1968. 136 numb. leaves.

93. Way, K. et al. (eds.) Nuclear data sheets NRC 61-2-2. Washington, D. C. National Academy of Sciences, 1961.

94. Way, K. et al. (eds.) Nuclear Data 1(1):B1-1-11-B1-1-24. 1966.

95. White, Gladys. X-ray attenuation coefficients from 10 keV to 100 MeV. Washington, D. C. National Bureau of Standards, 1957. 54 p. (National Bureau of Standards Circular 583.)

96. Wood, G. T. et al. Analysis of gamma-gamma cascades by polarization and directional correlation: Decay of Rh^{101g}. Physical Review 150:956-963. 1966.